Dynamics of dipolar ferromagnets below T_c

H. Schinz
sd&m software design & management GmbH & Co. KG, Thomas-Dehler-Straße 27, D-81737 München, Germany

F. Schwabl
Institut für Theoretische Physik, Technische Universität München, James-Franck Straße, D-85747 Garching, Germany

(Received 22 July 1997)

We employ mode-coupling theory to determine the dynamic critical behavior of isotropic Heisenberg ferromagnets below the Curie temperature including the dipolar interaction. Mode-coupling equations are derived and solved self-consistently for the temperature and wave vector dependence of the dynamical response functions and line widths of the excitations of this model. Thus, earlier applications of the mode-coupling theory to the low-temperature phase of ferromagnets are generalized beyond the isotropic limit and the following detailed results are obtained. (1) Our expression for the spin-wave frequency agrees with spin-wave theory in the common range of validity. The frequency is higher than the isotropic limit. This enhancement depends on the angle between the magnetization $\vec{M}$ and the wave vector $\vec{q}$. The largest deviations occur when $\vec{q}$ is perpendicular to $\vec{M}$. The wave-vector dependence can be described by a pseudogap for larger values of the wave vector. For small q, the dispersion is modified from quadratic to linear in q. This goes in hand with the number of Goldstone modes being reduced from 2 to 1 upon inclusion of the dipolar interaction. Some indications for this behavior are discussed in an analysis of experiments on EuO and Ni. (2) As in the paramagnetic case, the dipolar interaction also leads to important qualitative changes in the scaling functions for the damping of the excitations. Both transverse and longitudinal damping are greater in the isotropic case with an angular dependence on $\vec{q}$ relative to $\vec{M}$. The transverse scaling function exhibits a pronounced minimum, which agrees with experiments performed on EuO. In contrast the data cannot be explained by the isotropic transverse scaling function which decreases monotonically. The longitudinal damping shows a crossover at $q \approx q_D$ from $q^{5/2}$ to a noncritical q^0 behavior. The width of the central spin relaxation peak exceeds the spin-wave energy and polarized neutrons are required for its detection. The temperature variation of both quantities is similar to the paramagnetic case. (3) The competition of the dipolar interaction and the exchange interaction, characterized by the direction of the wave vector and the spontaneous magnetization, respectively, gives rise to a severe reduction of symmetry and a complicated tensorial structure of the equations. We identify the three important orthogonal directions, which correspond to the longitudinal and the two transverse excitations (spin waves). (4) Finally, we show that our results compare favorably with experiments on EuO and Ni. [S0163-1829(98)02813-6]

I. INTRODUCTION

During the recent years, the accuracy of experiments on the critical dynamics of magnetic systems increased considerably. Due to experimental progress primarily in neutron scattering, it has now become possible to investigate these systems in great detail. The use of polarized neutrons makes it possible to distinguish between different contributions to the neutron scattering cross section.[1–3] (See also, Refs. 4, 5.) The method of neutron spin-echo measurements allows to cover regions of very small wave vectors and to probe the time dependence, i.e., the line shape.[6] With electron spin resonance and nuclear magnetic resonance,[7–10] one measures the frequency properties at vanishing wave vector.

What can theory contribute to this progress in our understanding of these systems? In an intense and close interplay between experiment and theory over several years, mode-coupling theory proved to be the most successful approach for quantitatively describing the experimental findings.[11–13] With this theory, it is possible to calculate the damping rates, i.e., the *linewidths*, and even the *line shapes* of the dynamic excitations. It became clear in these investigations, that the dipolar interaction cannot be neglected for these systems for $T > T_c$.

In this paper, therefore, our aim is to generalize the theory to temperatures below T_c, including the dipolar interaction. We calculate the dynamic critical properties of isotropic Heisenberg ferromagnets, i.e., we calculate the scaling functions of the damping.

Now, we want to discuss briefly the two essential physical aspects, relevant for our calculation, and the results to be expected from that. Why is the dipolar interaction so important for critical phenomena, although it is so weak and can often be neglected? (Its strength corresponds to 10 to 100 mK while typical Curie temperatures range from 10 to 1000 K.) This can be ascribed to the following four properties of the dipolar interaction. (1) It is of long range (in contrast to the short-range exchange interaction) and therefore determines the asymptotic critical properties as the correlation length diverges. (2) It is anisotropic introducing the direction of the wave vector as a preferred direction. This leads to additional angular dependencies. (3) It breaks rotation invari-

ance, thereby lowering the symmetry, and influencing the dynamics of the order parameter markedly. (4) It introduces a second length scale in addition to the correlation length, the so called dipolar wave vector. This leads to generalized scaling laws. This second temperature-independent ''mass'' also suppresses fluctuations.

Besides the dipolar interaction, a second aspect is very relevant for the critical dynamics below T_c: The occurrence of Goldstone modes due to the spontaneously broken symmetry. These excitations are massless and therefore have a considerable influence on the properties of the system. Their fluctuations make the system ''critical'' in the whole low-temperature phase. With great effort it has been tried to tackle the problems connected with these massless modes by renormalization group theory (e.g., in Refs. 14, 15). But the analytic effort is rather high and this approach always relies on a perturbation series. It is therefore very attractive to try a nonperturbation-theory based approach, the mode-coupling theory.

Combining the dipolar interaction and the Goldstone modes, it is a very important observation, that the Goldstone fluctuations are not completely eliminated due to the dipolar interaction but rather their number is reduced by 1. This reduction from 2 in the isotropic case to 1 can be obtained from hydrodynamic considerations,[16] from spin-wave theories,[17–19] or from renormalization-group theory.[20] See also Ref. 21. The continuous symmetry, which leads to the one remaining Goldstone mode, is the invariance of the Hamiltonian against infinitesimal rotations of the spontaneous magnetization $\vec{M}$ around the direction of the wave vector $\vec{q}$. One single exception occurs when the wave vector $\vec{q}$ is oriented parallel to the magnetization $\vec{M}$. Then, two Goldstone modes survive and only the longitudinal mode in the direction of $\vec{q}$ and $\vec{M}$ is modified by the dipolar interaction.

What is to be expected from these observations? (Here, we only highlight some of the results.) (1) Including the dipolar interaction, the magnetization is no longer conserved. Therefore it comes as no surprise that the linewidths are increased, which is equivalent to enhanced damping or shortened lifetime. (2) It is also quite clear that the corresponding scaling functions depend on the relative orientation between the magnetization and the wave vector, characterizing the dipolar interaction. Therefore, a very complicated tensorial structure for the three excitations arises, which makes it both difficult to present the theoretical results, and to measure the proper quantities for comparison with theory. (3) Certainly the most striking effect of the dipolar interaction on the critical dynamics of ferromagnets is that the transverse scaling function shows a distinct minimum. This is in marked contrast to the isotropic case, where the scaling function decays monotonically. (4) For completeness we shortly mention the effects of the dipolar interaction on the spin-wave frequency. There is an increase (describable by a pseudogap for large wave vectors), an angular dependence, and, most prominently, an altered asymptotic behavior for small wave vectors. The dispersion is now linear in q instead of quadratic.

Now, we give a brief account of earlier theories. Calculations including the dipolar interaction in the framework of spin-wave theory were performed in Refs. 18, 22, 19. In Ref. 23 the authors tried to cope with the dipolar interaction in perturbation theory using a diagrammatic technique. (See also, Ref. 24.) These approaches are, however, not capable of dealing with critical phenomena. An attempt to use mode-coupling theory for the description of critical dynamics in a dipolar ferromagnet was undertaken in Ref. 25. They, however, used many approximations concerning the mode-coupling equations as well as the static susceptibilities (see the more detailed discussion below). In Ref. 26 was reported a calculation based on the non-self-consistent analysis of mode-coupling equations, which also contain a number of approximations (see below). Here, many of these approximations are eliminated, and the equations are solved self-consistently.

To give a short overview over different approaches to treat the dynamic properties of isotropic Heisenberg ferromagnets, we mention early renormalization group calculations[27,28] and macroscopic spin-wave theories.[29,30] Results have also been achieved by using diagrammatic techniques[31] and using mode-coupling theory in a non-self-consistent manner.[32,33] See also Ref. 34. The corresponding mode-coupling equations have been derived microscopically in Ref. 35. In some limiting cases they have been solved analytically in Ref. 36. In Ref. 11 they were solved numerically in the general case. One approach is the numerical simulation of finite systems. The results then have to be extrapolated to the thermodynamic limit via finite-size scaling analysis. In Ref. 37 the isotropic Heisenberg ferromagnet on a bcc lattice was investigated near T_c. It was found that the dynamical scaling hypothesis holds and the dynamic critical exponent $z=2.478(28)$ agrees with theoretical predictions. A more comprehensive review can be found in Ref. 13.

The outline of this article is as follows. In the course of setting up the mode-coupling equations and their scaling form for the dipolar ferromagnet in Sec. IV, we introduce the Hamiltonian in Sec. II and briefly sketch the theory in Sec. III. Some elements of the theory, which have to be provided independently, the static susceptibilities and the so-called frequency matrix, are covered more closely in Appendixes A and B. In Sec. V we discuss several possibilities to assume a line shape, the so called Lorentzian approximation. Here, such an approximation is not straightforward because of the complicated tensorial structure of the problem. In Appendix C we therefore present an alternative formulation, while Appendix D contains some details of the calculation. In Sec. VI, after a short description of the numerical method to solve the coupled integrodifferential equations, we present the central results of our calculations, the linewidths for the different modes. These are compared with experimental measurements for the strongly dipolar magnet EuO and the weakly dipolar magnet Ni in Sec. VII. Section VIII contains the summary and conclusions.

II. HAMILTONIAN

The Hamiltonian for the spin operators $\vec{S}_i$ located at lattice sites i with Cartesian components $\alpha,\beta=x,y,z$ is given by[38]

$$H=-\sum_{i,j} U_{ij}^{\alpha\beta} S_i^{\alpha} S_j^{\beta}, \tag{1a}$$

TABLE I. The configuration number c, the coefficient a_1, and the volume ratio b^2 for simple cubic (sc), body centered cubic (bcc), and face centered cubic (fcc) lattices. See text.

	sc	bcc	fcc
c	6	8	12
a_1	4π	$3\pi\sqrt{3}$	$4\pi\sqrt{2}$
$a^3/v =: b^2$	1	2	4

$$U_{ij}^{\alpha\beta}=\frac{1}{2}\,\hat{J}\,\delta_{\alpha\beta}\delta_{j,i+\delta}-(1-\delta_{ij})G\,\frac{\partial^2}{\partial R_i^\alpha \partial R_j^\beta}\,\frac{1}{|\vec{R}_i-\vec{R}_j|}. \tag{1b}$$

Here, the exchange interaction $\hat{J}$ is restricted to nearest neighbors $\delta=NN$ and the strength of the dipolar interaction is given by $G=\frac{1}{2}(g_L\mu_B)^2$ with the Landé factor g_L and the Bohr magneton μ_B. Performing an Ewald summation of the dipolar interaction the Hamiltonian can be transformed into wave-vector space. Restricting ourselves to the leading order in the wave vector $\vec{q}$ we end up with the following expression:[38]

$$H=\int_{\vec{q}} U_{\vec{q}}^{\alpha\beta} S_{\vec{q}}^{\alpha} S_{-\vec{q}}^{\beta}, \tag{2a}$$

$$U_{\vec{q}}^{\alpha\beta}=-J_0\cdot\delta^{\alpha\beta}+J\left\{q^2a^2\delta^{\alpha\beta}+g\,\frac{q^\alpha q^\beta}{q^2}\right\}. \tag{2b}$$

The lattice constant of the conventional (cubic) unit cell is denoted by a, while v is the volume of the primitive unit cell (containing only one atom). For different Bravais lattices the number of atoms per cubic unit cell differs and thus $b=\sqrt{a^3/v}$ depends on the lattice type (see Table I and Ref. 39). Later on, we will measure lengths in units of a. The notation $\int_{\vec{q}}$ is an abbreviation for

$$\int_{\vec{q}}=\int v\,\frac{d^3q}{(2\pi)^3}. \tag{3}$$

In principle, this integral extends only over the first Brillouin zone, but since we are interested in critical phenomena and hence in small wave vectors, we can extend the integration to infinity. For larger values of q nonuniversal dependencies on the form and the size of the Brillouin zone would enter. Then, however, also other (microscopic and nonuniversal) mechanisms and interactions besides the ones included have to be taken into account. The expansion of the Fourier transformed exchange interaction leads to the coefficients J_0 and J. The former will not enter the equations of motion (see below) while the latter is given by $J=(c/6)\hat{J}$, neglecting small corrections due to the dipolar interaction (we used $G/\hat{J}a^d\ll 1$). By c we denote the configuration number, i.e., the number of nearest neighbors (see Table I). Finally, we introduced the dimensionless quantity g related to the dipolar wave vector q_D as a measure for the relative strength of the dipolar interaction compared to the exchange interaction[11,39]

$$g=(q_Da)^2=\frac{a_1G}{Ja^3}\left(\frac{c}{6}\right)^{3/2}. \tag{4}$$

The coefficient a_1 stems from the Ewald summation of the dipolar interaction and depends also on the lattice type (Table I and Ref. 38).

III. GENERAL MODE-COUPLING THEORY

We now proceed with a brief description of the mode-coupling theory. This theory has been invented for the description of fluids[40] and was thereafter extended and successfully applied to several other problems,[41–43,13] including nonequilibrium thermodynamics.[44,45] More detailed presentations can be found in Refs. 11–13, 46, 47, and references therein. For the more general aspects consider also Refs. 48–50 and 51.

The main observation in the derivation of our mode-coupling equations is the existence of time scale separation. Due to conservation laws the collective hydrodynamic modes become slow when the wave vector tends to zero. Also, in the vicinity of second order phase transitions the order parameter modes become slow (''critical slowing down''). Projecting out the remaining fast variables[52,53] one arrives at generalized Langevin equations with explicit expressions for the damping Γ (non local in time, thus incorporating memory effects) and for the ''random'' forces. Below T_c there is in addition a reversible time dependence (corresponding to propagating modes) which is described by a frequency matrix ω. These Langevin equations are formally exact, but to be physically meaningful it is essential to pick the right variables for the set of slow variables $\{A_\mu\}$. Theoretically it is convenient to introduce the Kubo relaxation function ϕ ($\hbar=1$)

$$\phi^{\mu\nu}(\vec{q},t)=\int_0^\beta d\lambda\langle e^{\lambda H}\delta A_\mu(\vec{q},t)e^{-\lambda H}\delta A_\nu^\dagger(\vec{q},0)\rangle$$

$$=i\lim_{\varepsilon\to 0}\int_t^\infty e^{-\varepsilon\tau}\langle[A_\mu(\vec{q},\tau),A_\nu^\dagger(\vec{q},0)]\rangle d\tau, \tag{5}$$

where β is the inverse temperature $1/k_BT$ and $\delta A_\mu := A_\mu-\langle A_\mu\rangle$. Equivalently, it can be expressed by the spin-spin correlation function or the dynamic (frequency dependent) susceptibility. It has the property

$$\phi^{\mu\nu}(\vec{q},t=0)=\chi^{\mu\nu}(\vec{q},\omega=0), \tag{6}$$

i.e., the relaxation function at time $t=0$ equals the static susceptibility tensor. Using this quantity as the scalar product

$$(A|B):=\phi^{AB}(\vec{q},t=0), \tag{7}$$

we can define orthonormal variables $X_\mu=A_\mu/\sqrt{\chi_{\vec{q}}^{\mu}}$ and obtain the equation of motion for the Kubo relaxation function

$$\frac{\partial}{\partial t}\phi^{\mu\nu}(\vec{q},t)=i\omega_{\mu\kappa}(\vec{q})\phi^{\kappa\nu}(\vec{q},t)$$

$$-\int_0^t\Gamma_{\mu\kappa}(\vec{q},t')\phi^{\kappa\nu}(\vec{q},t-t')\,dt', \tag{8}$$

with frequency and damping matrix given by

$$\omega_{\mu\nu}=-i(\dot{X}_\mu|X_\nu)=-\langle[X_\mu,X_\nu^\dagger]\rangle, \tag{9}$$

$$\Gamma_{\mu\nu}(t)=(f_\mu(t)|f_\nu(0)). \tag{10}$$

The random force f

$$f_\mu(t)=e^{iQ\mathcal{L}t}Q\dot{X}_\mu \tag{11}$$

develops in time according to the Liouville operator $\mathcal{L}$ projected onto the fast variables by means of the projection operator Q. Applying the half-sided Fourier transform and using the property (6) we get the first part of the mode-coupling equations

$$\phi(\vec{q},\omega):=\int_0^\infty e^{i\omega t}\phi(\vec{q},t)dt=i\sqrt{\chi_{\vec{q}}}\,\frac{1}{\omega\mathbf{1}+\omega_{\vec{q}}+i\Gamma(\vec{q},\omega)}\,\sqrt{\chi_{\vec{q}}}, \tag{12}$$

which allows one to compute ϕ for known Γ.

In order to proceed, we have to make two approximations for Γ. At first we replace Γ by

$$\Gamma(t)\approx(\dot{X}(t)|\dot{X}(0)). \tag{13}$$

This can be justified, e.g., if A_μ is conserved and one sticks to small wave vectors.[50] If now the time derivative of X is given by some functional of X,

$$\dot{X}_\mu=\mathcal{F}(\{X_\nu\}), \tag{14}$$

Γ can be expressed by some higher order relaxation functions. To close this open hierarchy of equations, we apply the factorization approximation, which replaces a higher order relaxation function by the sum of all possible contractions (products of the simple relaxation functions) in a procedure similar to the random-phase approximation (RPA). This corresponds to neglecting multimode decays in a perturbation theory. It can be justified in the limit of vanishing wave vector,[13] since then the relative contribution of the corresponding diagrams tends to zero. Another class of diagrams would lead to vertex corrections, which would yield a finite value for the Fisher exponent η.[13] Thus we obtain the final equation connecting the memory matrix Γ back to the relaxation function ϕ:

$$\Gamma\approx\mathcal{G}(\{\phi\}). \tag{15}$$

Equations (12) and (15) define the self-consistency problem to be solved. The specific model enters these general mode-coupling equations at three places. For the calculation of the frequency matrix (9) we need model-dependent thermodynamic expectation values, we need the static susceptibilities (6), which cannot be taken from mode-coupling theory, and finally for the time evolution of the slow variables (14) we need some model specific prescription.

For ferromagnets the relevant slow variables are the spin densities and we can use the ''microscopic'' Heisenberg equations of motion

$$\dot{X}_\mu=i[H,X_\mu] \tag{16}$$

for Eq. (14). Using the spin-commutation rules in Cartesian coordinates this yields in direct space

$$\partial_t S_i^\alpha=\varepsilon_{\alpha\beta\gamma}\{S_i^\beta U_{ij}^{\gamma\delta}S_j^\delta-U_{ij}^{\beta\delta}S_j^\delta S_i^\gamma\}, \tag{17}$$

with the interaction U given in Eq. (1b). This symmetric cross product transforms to

$$\partial_t S_{\vec{q}}^\alpha=\varepsilon_{\alpha\beta\gamma}\int_{\vec{q}'}U^{\beta\delta}(\vec{q}')\{S_{\vec{q}'}^\delta,S_{\vec{q}-\vec{q}'}^\gamma\} \tag{18}$$

in $\vec{q}$ space, using {,} for the quantum mechanical anticommutator. From (2) it is obvious that in the isotropic limit (without dipolar interaction) $S_{\vec{q}}$ does not change in time for vanishing q, corresponding to a conserved order parameter, while in the general dipolar case, the time derivative attains a finite value and the homogeneous magnetization is no longer conserved.

IV. MODE-COUPLING EQUATIONS FOR $T<T_C$

In the further development of the calculation it is convenient to use orthogonalized modes. As is clear from Eq. (6), we need the static susceptibility tensor, which has to be diagonalized. The corresponding eigenvectors then determine the coordinate system which we will use. The derivation of these susceptibilities is quite involved[21] and we only quote the main results in Appendix A. The eigenvectors depend in a fairly complicated manner on the relative orientation of the wave vector $\vec{q}$ and the magnetization $\vec{M}$. This is the main source for the considerably increased complexity as compared to the isotropic case or the calculations above the Curie temperature T_c.

The results in Appendix A are given in scaling form. Instead of wave vector q, correlation length ξ (below T_c), and dipolar wave vector q_D we use scaling variables x,y and alternatively the corresponding polar coordinates R, ϕ according to

$$x=\frac{\sqrt{r_L}}{q}=\frac{1}{q\xi},\quad y=\frac{\sqrt{g}}{q}=\frac{q_D}{q},$$

$$R=\sqrt{x^2+y^2}=\frac{\sqrt{\xi^{-2}+q_D^2}}{q},\quad \tan\phi=\frac{y}{x}=\sqrt{\frac{g}{r_L}}=q_D\xi. \tag{19}$$

The variable ϕ is a measure for temperature while R accounts for the wave vector (at fixed temperature). Furthermore, we introduce the angle ϑ between the wave vector $\vec{q}$ and the plane perpendicular to the magnetization $\vec{M}$. $\vartheta=0°$ corresponds to in-plane orientation of $\vec{q}$ while for $\vartheta=90°$ the wave vector $\vec{q}$ is perpendicular to the plane. A formal definition is given in Appendix A, Eq. (A3).

With this choice of the coordinate system we get the following equations of motion:

$$\partial_t S_{\vec{q}}^i=\int_{\vec{q}'}\frac{1}{2}\,V_{ikl}(\vec{q}',\vec{q}-\vec{q}')\{S_{\vec{q}'}^k,S_{\vec{q}-\vec{q}'}^l\} \tag{20}$$

with the vertices

$$V_{ikl}(\vec{q}',\vec{q}-\vec{q}')=E_{ijl}(\vec{q}',\vec{q}-\vec{q}')U^{jk}(\vec{q}')-E_{ikj}(\vec{q}',\vec{q}-\vec{q}')U^{jl}(\vec{q}-\vec{q}'). \tag{21}$$

The fully antisymmetric tensor $\varepsilon_{\alpha\beta\gamma}$ in Eq. (18) is thus replaced by

$$E_{ijk}(\vec{q}',\vec{q}-\vec{q}')=\vec{v}_i(\vec{q})[\vec{v}_j(\vec{q}')\times\vec{v}_k(\vec{q}-\vec{q}')]. \quad (22)$$

The matrix $U^{jk}(\vec{q})$ mediating the spin-spin interaction in this coordinate system is given by

$$U^{jk}(\vec{q})=\vec{v}_j^{\,T}(\vec{q})U(\vec{q})\vec{v}_k(\vec{q})=Jq^2\mathbf{1}^{jk}+Jg\hat{M}^{jk}(\phi,\vartheta),$$

$$\hat{M}^{jk}(\phi,\vartheta)=:\hat{m}^j\cdot\hat{m}^k,\quad \vec{\hat{m}}(\phi,\vartheta)=\begin{pmatrix}0\\ \sqrt{\tilde{u}}\\ \sqrt{1-\tilde{u}}\end{pmatrix}, \quad (23)$$

$$\tilde{u}(\phi,\vartheta)=\cos^2\,\varphi_3(90^\circ-\phi,\vartheta).$$

The eigenvectors $\vec{v}_i$ of the static susceptibility tensor and the angle φ_3 are defined in Appendix A. These expressions can now be inserted into Eq. (13) and after carrying out the factorization approximation we get the final expression for the damping matrix Γ in terms of the relaxation matrix ϕ:

$$\Gamma^{ij}(\vec{q},t)=\frac{1}{\sqrt{\chi^i_{\vec{q}}\chi^j_{\vec{q}}}}(\dot{S}^i_{\vec{q}}(t)|\dot{S}^j_{\vec{q}})$$

$$=\frac{4k_BT}{\sqrt{\chi^i_{\vec{q}}\chi^j_{\vec{q}}}}\int_{\vec{q}'}\frac{1}{2}\,T'_{ijkmln}(\vec{q}',\vec{q}-\vec{q})$$

$$\times\phi^{km}(\vec{q}',t)\phi^{ln}(\vec{q}-\vec{q}',t), \quad (24)$$

where we introduced the kernel

$$T'_{ijkmln}(\vec{q}',\vec{q}-\vec{q}')=V_{ikl}(\vec{q}',\vec{q}-\vec{q}')V_{jmn}(\vec{q}',\vec{q}-\vec{q}'). \quad (25)$$

Equation (24) together with Eq. (12) has now to be solved for the relaxation function ϕ.

At this point we compare with two previous treatments of the problem. The equations used in Ref. 25 differ from ours in several respects. The anisotropy in $\vec{q}$ of the static susceptibility χ has been neglected. Also, these authors did not include the coexistence anomaly in the longitudinal susceptibility, ($\chi_L\sim 1/q$ for $q\to 0$). By averaging over all directions of the wave vector the tonsorial character of the problem was eliminated and thus the equations were reduced to scalar quantities. Finally, only the parameters of a particular parametrization of the linewidths and not the complete functions have been derived self-consistently. Therefore, only some aspects of the dipolar interaction are included in this work.

The mode-coupling equations used in Ref. 26 also contain a number of severe approximations. The dispersion relation is valid only for not too small wave vectors. The static susceptibilities do not account for the dipolar crossover, and especially neglect the complicated tonsorial structure. As the treatment of Raghavan and Huber, the results of Lovesey are therefore restricted to the weak dipolar region $q_D\xi\ll 1$. This is also due to the assumed diagonality of the damping matrix in terms of the spin fluctuations parallel and perpendicular to the magnetization, which certainly does not hold in the region $q_D\xi>1$ and especially not at $T=T_c$, where the longitudinal mode is parallel to the wave vector $\vec{q}$ and not to the magnetization. Since the dipolar interaction is not incorporated properly and, therefore, small wave vectors cannot be considered, the applicability of the results to critical phenomena is very restricted. Finally, even these simplified equations have not been solved self-consistently but rather in a first iteration based on the neglection of the damping.

Before we derive the scaling form of the mode-coupling equations we have to deal with the frequency matrix in Eq. (12). Again, it is helpful to use the coordinate system where the static susceptibility is diagonal, i.e., to use the directions of the eigenvectors $\vec{v}_i(\vec{q})$ instead of the Cartesian coordinates (indices $i=1,2,3$ instead of $\alpha=x,y,z$). Then, the frequency matrix (9) can be calculated according to

$$C^{ij}_{\vec{q}}:=-\omega^{ij}_{\vec{q}}=\frac{1}{\sqrt{\chi^i_{\vec{q}}\chi^j_{\vec{q}}}}\langle[S^i_{\vec{q}},S^j_{-\vec{q}}]\rangle. \quad (26)$$

The details of the calculation can be found in Appendix B. The eigenvalues of this matrix are 0, $\omega_{\vec{q}}$, and $-\omega_{\vec{q}}$. The first important result is the observation that the frequency matrix is not diagonal together with the tensor of the static susceptibility. The eigenvectors of $C_{\vec{q}}$ do not coincide with the eigenvectors of χ. This will cause the major difficulties in the solution of the mode-coupling equations and increase the effort considerably.

The second important result is an expression for the spin-wave frequency

$$\omega_{\vec{q}}=2Jm\sqrt{q^2(q^2+q_D^2\,\cos^2\,\vartheta)}. \quad (27)$$

Equation (27) generalizes spin-wave results up to T_c. It is identical with the expression obtained by spin-wave theory[54,30] if one replaces the thermodynamic expectation value $m=\langle S^z_0\rangle$ by the classical $T=0$ value S. Spin-wave theory can, however, be improved[55] to also yield $\langle S^z_0\rangle$ instead of S. The spin-wave frequency (27) is now angle dependent and increased compared to the isotropic case. For $\vartheta=90^\circ$ ($\vec{q}\|\vec{M}$) the effect of the dipolar interaction is eliminated and we recover the isotropic spin-wave dispersion relation. In the general case there is a ''mass term,'' which has several consequences. For small q it modifies the dispersion which is now linear instead of quadratic. We get

$$\omega_{\vec{q}}\approx 2Jm(qq_D\,\cos\,\vartheta+q^2),\quad q\ll q_D\,\cos\,\vartheta. \quad (28)$$

Thus, the spin-wave energies are strongly increased but there is still no gap in the spectrum. This corresponds to the one remaining Goldstone mode in the dipolar case, which leads to massless excitations. For large q the mass term leads to a pseudogap, i.e., the spin-wave frequency appears to have been shifted upwards:

$$\omega_{\vec{q}}\approx 2Jm\left(q^2+\frac{1}{2}q_D^2\,\cos^2\,\vartheta\right),\quad q\gg q_D\,\cos\,\vartheta. \quad (29)$$

Both asymptotic expressions together with the complete formula (27) are shown in the left part of Fig. 1 for $\vartheta=0^\circ$. In the right part we show the spin-wave frequency for various values of ϑ.

Next, we derive from Eqs. (24) and (12) the mode-coupling equations in scaling form, which will serve as the

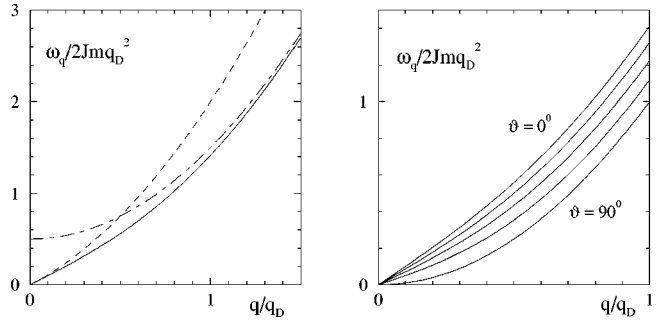

FIG. 1. Spin-wave frequency $\omega_{\vec{q}}$ of the dipolar ferromagnet vs wave vector q. Left: $\vartheta=0°$, general formula (—), approximation for small (––), and large (-··-) wave vectors q. Right: $\vartheta=0°$, 30°, 45°, 60°, 90° (as indicated in the graph), where ϑ is the angle enclosed by $\vec{q}$ and the plane perpendicular to $\vec{M}$.

starting point for the numerical solution. At first we give the scaling form for the spin-wave frequency. By inspection of Eq. (27) we get

$$\omega_{\vec{q}}(\xi,g)=F'q^z\cdot\hat{\omega}'(x,y,\vartheta),$$

$$\hat{\omega}'(x,y,\vartheta)=\sqrt{x(1+y^2\cos^2\vartheta)}, \tag{30}$$

where $z=5/2$ is the dynamic critical exponent. Strictly speaking the exact result for the isotropic Heisenberg ferromagnet is[56]

$$z=\frac{d}{2}+1-\frac{\eta}{2}. \tag{31}$$

But since η is quite small [e.g., $\eta=0.04$ for the isotropic n-vector model in $d=n=3$ in $O(\epsilon^2)$ (Ref. 57)], we can safely neglect it here.

The static susceptibilities have already been given in scaling form in Eqs. (A1)–(A6). The general form of the scaling laws connected with static quantities is (again setting to zero the Fisher exponent η)

$$\chi^i_{\vec{q}}(\xi,g)=\chi_0 q^{-2}\cdot\hat{\chi}^i(x,y,\vartheta_{\vec{q}}),$$

$$C^{ij}_{\vec{q}}(\xi,g)=-Fq^z\cdot\tilde{\omega}^{ij}(x,y,\vartheta_{\vec{q}}). \tag{32}$$

Here, we used the polar angle $\vartheta_{\vec{q}}$ of $\vec{q}$. Because of the invariance of the Hamiltonian against $\vec{q}\to-\vec{q}$ it can later be replaced by the angle ϑ as defined in Eq. (A3). The quantities do not depend on the angle φ, which reflects the symmetry belonging to the one remaining Goldstone mode. For the dynamic quantities we have in Fourier space

$$\Gamma^{ij}(\vec{q},\omega,\xi,g)=Fq^z\gamma^{ij}(x,y,\nu,\vartheta_{\vec{q}}),$$

$$\phi^{ij}(\vec{q},\omega,\xi,g)=\frac{\chi_0 q^{-2}}{Fq^z}\varphi^{ij}(x,y,\nu,\vartheta_{\vec{q}}), \tag{33}$$

with $\omega=Fq^z\nu$ and as a function of time

$$\Gamma^{ij}(\vec{q},t,\xi,g)=[Fq^z]^2G^{ij}(x,y,\tau,\vartheta_{\vec{q}}),$$

$$\phi^{ij}(\vec{q},t,\xi,g)=\chi_0 q^{-2}\varphi^{ij}(x,y,\tau,\vartheta_{\vec{q}}), \tag{34}$$

with

$$t=\frac{1}{Fq^z\tau}.$$

The scaling variable $\vec{\kappa}=\vec{q}'/q$ and the corresponding polar coordinates κ, ϑ', and φ' will substitute the integration variable $\vec{q}'$ in Eq. (24).

Since there are two different non universal amplitudes F and F' in Eqs. (30) and (32)–(34), it is important to know whether the ratio $\hat{b}=F'/F$ is universal or not. In Ref. 58 and in more detail in Ref. 59, it has been shown that $\hat{b}$ is universal (which could also be confirmed experimentally for various magnets[58]) and that its value is roughly $\hat{b}\approx 7.0-9.4$.

Finally, the kernels in Eq. (25) scale as

$$T'_{ijkmln}(\xi,g,\vec{q}',\vec{q}-\vec{q}')=J^2\vec{q}'^2(\vec{q}-\vec{q}')^2 t'_{ijkmln}(x,y,\vartheta_{\vec{q}},\vec{\kappa}), \tag{35}$$

with the scaling function

$$t'_{ijkmln}(x,y,\vartheta_{\vec{q}},\vec{\kappa})=v_{ikl}(x,y,\vartheta_{\vec{q}},\vec{\kappa})v_{jmn}(x,y,\vartheta_{\vec{q}},\vec{\kappa})$$
$$=:\frac{w_{ijkmln}(x,y,\vartheta_{\vec{q}},\vec{\kappa})}{\kappa^2\kappa_-^2},$$

$$v_{ikl}(x,y,\vartheta,\vartheta',\Delta\varphi',\kappa)$$
$$=\frac{2\kappa\ \eta-1}{\kappa\kappa_-}E_{ikl}\left(\frac{x}{y},\vartheta,\vartheta',\Delta\varphi',\kappa\right)$$
$$+\frac{y^2}{\kappa\kappa_-}\left\{E_{ipl}\left(\frac{x}{y},\vartheta,\vartheta',\Delta\varphi',\kappa\right)\hat{M}^{pk}\left(\frac{x}{y},\vartheta'\right)\right.$$
$$\left.+E_{ipk}\left(\frac{x}{y},\vartheta,\vartheta'',\Delta\varphi'',\kappa_-\right)\hat{M}^{pl}\left(\frac{x}{y},\vartheta''\right)\right\}. \tag{36}$$

The quantities φ'', ϑ'', and κ_- are defined in Appendix A. The tensors E and $\hat{M}$ have been defined in Eqs. (22) and (23), respectively.

With Eqs. (24) and (12) the complete final mode-coupling equations in scaling form for the scaling functions G and φ are then given by

$$G^{ij}(x,y,\vartheta,\tau)=\frac{1}{4}\hat{c}\int\frac{d^3\kappa}{(2\pi)^3}\frac{1}{\sqrt{\hat{\chi}^i(x,y,\vartheta)\hat{\chi}^j(x,y,\vartheta)}}$$
$$\times t'_{ijkmln}(x,y,\vartheta,\vec{\kappa})\varphi^{km}\left(\frac{x}{\kappa},\frac{y}{\kappa},\vartheta',\kappa^z\tau\right)$$
$$\times\varphi^{ln}\left(\frac{x}{\kappa_-},\frac{y}{\kappa_-},\vartheta'',\kappa_-^z\tau\right) \tag{37}$$

and

$$\varphi^{ij}(x,y,\vartheta,\nu)=i\sqrt{\hat{\chi}^i(x,y,\vartheta)\hat{\chi}^j(x,y,\vartheta)}$$
$$\times\left[\frac{1}{\nu\mathbf{1}+\tilde{\omega}(x,y,\vartheta)+iG(x,y,\vartheta,\nu)}\right]^{ij}. \tag{38}$$

The transition from time to frequency in Eq. (38) is achieved by a half-sided Fourier transform

$$\varphi(\nu)=\int_0^\infty e^{i\nu\tau}\varphi(\tau)d\tau. \tag{39}$$

With $z=5/2$ following from general scaling considerations [Eq. (31)] and

$$F=\sqrt{\frac{8\chi_0 J^2 k_B T}{\hat{c}}}=\sqrt{\frac{4Jk_B T}{\hat{c}}}, \tag{40}$$

the q and ω dependencies in the mode-coupling equations are such that we get a dimensionless scaling law. Because of the second scaling variable y one has to distinguish, however, between this formal exponent and the ''real'' effective exponent $z_{\rm eff}$. For example, there is a crossover from $z_{\rm eff}=5/2$ to $z_{\rm eff}=2$ for the transverse and to $z_{\rm eff}=0$ for the longitudinal linewidth as one approaches T_c from above.[11] The numerical constant b in the nonuniversal amplitude F depends on the lattice type and is tabulated in Table I. The universal constant $\hat{c}$ fixes the global numerical scale of the scaling functions, which can be chosen arbitrarily. For example, for $\hat{c}=8\pi^4$ we get for the damping at T_c in Lorentzian approximation[11]

$$G^{ij}_{LLN}(x=0,y=0)\approx 5.1326\,\delta^{ij} \quad \text{for} \quad \hat{c}=8\pi^4. \tag{41}$$

For $\hat{c}\approx 8\pi^4/(5.1326)^{239}$ the corresponding scaling function is normalized to unity:

$$G^{ij}_{LLN}(x=0,y=0)=1\,\delta^{ij} \ \text{ for } \ \hat{c}\approx\frac{8\pi^4}{(5.1326)^2}. \tag{42}$$

Therefore, we can arbitrarily shift numerical factors between $\hat{c}$ in the equations and the resulting scaling functions. In the following, we will choose $\hat{c}=8\pi^4$.

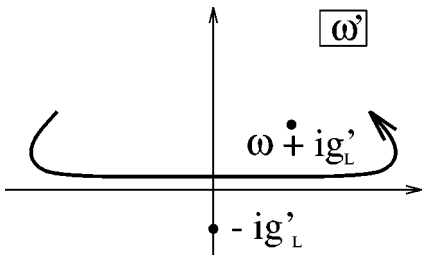

FIG. 2. Contour of integration of I'_{ab} in the complex ω' plane. Also shown are the poles of the integrand for I'_{LL}.

As a function of time, Eq. (38) becomes a differential equation for φ:

$$\frac{\partial}{\partial t}\varphi^{ij}(x,y,\vartheta,\tau) = \sum_k \sqrt{\frac{\hat{\chi}^i(x,y,\vartheta)}{\hat{\chi}^k(x,y,\vartheta)}}\left\{ i\tilde{\omega}^{ik}(x,y,\vartheta)\varphi^{kj}(x,y,\vartheta,\tau) - \int_0^\tau d\tau' G^{ik}(x,y,\vartheta,\tau')\varphi^{kj}(x,y,\vartheta,\tau-\tau')\right\}. \tag{43}$$

The initial condition at $\tau=0$ is given by the identity (6):

$$\varphi^{ij}(x,y,\vartheta,\tau=0)=\hat{\chi}^i(x,y,\vartheta)\,\delta^{ij}. \tag{44}$$

With the help of the convolution theorem

$$\int_0^\infty e^{i\nu\tau}f(a\tau)g(b\tau)d\tau = \int_{-\infty}^\infty \frac{d\nu'}{2\pi}\frac{1}{a}f\left(\frac{\nu'}{a}\right)\frac{1}{b}g\left(\frac{\nu-\nu'}{b}\right) a,b>0, \tag{45}$$

Eq. (37) can be transformed into Fourier space

$$G^{ij}(x,y,\vartheta,\nu)=\frac{1}{4}\hat{c}\int\frac{d^3\kappa}{(2\pi)^3}\frac{1}{\sqrt{\hat{\chi}^i(x,y,\vartheta)\hat{\chi}^j(x,y,\vartheta)}}t'_{ijkmln}(x,y,\vartheta,\vec{\kappa})\int_{-\infty}^\infty\frac{d\nu'}{2\pi}\frac{1}{\kappa^z} \times\varphi^{km}\left(\frac{x}{\kappa},\frac{y}{\kappa},\vartheta',\nu'/\kappa^z\right)\frac{1}{\kappa_-^z}\varphi^{ln}\left(\frac{x}{\kappa_-},\frac{y}{\kappa_-},\vartheta'',(\nu-\nu')/\kappa_-^z\right). \tag{46}$$

Eliminating ϕ via Eq. (38) we get a closed system of integral equations for the scaling function G in Fourier space:

$$G^{ij}(x,y,\vartheta,\nu)=-\frac{1}{4}\hat{c}\frac{1}{\sqrt{\hat{\chi}^i(x,y,\vartheta)\hat{\chi}^j(x,y,\vartheta)}}\int\frac{d^3\kappa}{(2\pi)^3}t'_{ijkmln}(x,y,\vartheta,\vec{\kappa}) \times\sqrt{\hat{\chi}^k\left(\frac{x}{\kappa},\frac{y}{\kappa},\vartheta'\right)\hat{\chi}^m\left(\frac{x}{\kappa},\frac{y}{\kappa},\vartheta'\right)\hat{\chi}^l\left(\frac{x}{\kappa_-},\frac{y}{\kappa_-},\vartheta''\right)\hat{\chi}^n\left(\frac{x}{\kappa_-},\frac{y}{\kappa_-},\vartheta''\right)}\int_{-\infty}^\infty\frac{d\nu'}{2\pi}\left\{\left(\nu\mathbf{1}+\kappa^z\left[\tilde{\omega}\left(\frac{x}{\kappa},\frac{y}{\kappa},\vartheta'\right)+iG\left(\frac{x}{\kappa},\frac{y}{\kappa},\vartheta',\frac{\nu'}{\kappa^z}\right)\right]\right)^{-1}\right\}^{km}\left\{\left((\nu-\nu')\mathbf{1}+\kappa_-^z\left[\tilde{\omega}\left(\frac{x}{\kappa_-},\frac{y}{\kappa_-},\vartheta''\right)+iG\left(\frac{x}{\kappa_-},\frac{y}{\kappa_-},\vartheta'',\frac{\nu-\nu'}{\kappa_-^z}\right)\right]\right)^{-1}\right\}^{ln}. \tag{47}$$

V. GENERALIZED LORENTZIAN APPROXIMATION

Equations (37) and (38) or their equivalents are very complicated because of the dependence on q and ω. A very successful idea to reduce the complexity has been the so-called Lorentzian approximation.[11] There, one assumes a frequency independent damping G in the relaxation function ϕ (38). This amounts to a Lorentzian in Fourier space or an exponential decay of ϕ in time. Now, the integration over frequency in Eq. (46) or equivalently Eq. (47) can be performed analytically. Thus, the implicit frequency dependence is eliminated and the theory is reduced to the computation of a wave-vector dependent linewidth. Often, this is sufficient for comparison with experiments, since line widths are easier to measure than line shapes.

Reformulating and generalizing this idea, we assume that the damping matrix in Eq. (38) varies only slowly with frequency so that approximately it can be set constant. Then, we have to diagonalize ϕ in order to carry out the integration. Compared to the isotropic case, there is, however, one major difficulty in the dipolar case: We do not know in advance how to diagonalize the damping matrix Γ. This can essentially be traced back [Eqs. (48) and (49)] to the fact that the tensor of the static susceptibility χ does not commute with the frequency matrix C. They cannot be diagonalized simultaneously. Therefore, the diagonalization of Γ has to be done self-consistently together with the determination of Γ itself. There are two possible solutions to this problem. In Appendix C we show how the theory can be formulated without specifying the exact diagonalizing transformation for Γ. Unfortunately, the resulting expressions become rather involved and cumbersome. Here, we prefer to use the second possibility, an approximate diagonalization of Γ to be explained in more detail at the end of this section and in Appendix D. The essential result will be that we can approximately use the coordinate system spanned by the eigenvectors of the static susceptibility tensor. But first we formulate the general Lorentzian theory.

Assuming that the the damping matrix $\Gamma(\vec{q})$ to be determined is independent of frequency we get

$$\phi(\vec{q},\omega)\approx i\sqrt{\chi_{\vec{q}}}M(\vec{q},\omega)\sqrt{\chi_{\vec{q}}}, \tag{48}$$

$$M^{-1}(\vec{q},\omega)=\omega\cdot\mathbf{1}-C_{\vec{q}}+i\Gamma(\vec{q}). \tag{49}$$

Let $T_{\vec{q}}$ be a transformation into a new coordinate system, which diagonalizes M (in general, $T_{\vec{q}}$ is not unitary, since M is not necessarily normal, $[M,M^{\dagger}]\neq 0$)

$$T_{\vec{q}}^{-1}M^{-1}(\vec{q},\omega)T_{\vec{q}}=\omega\cdot\mathbf{1}+ig'(\vec{q}),$$

$$g'^{ab}(\vec{q})=\begin{pmatrix} g'_L(\vec{q}) & 0 & 0 \\ 0 & g'_T(\vec{q}) & 0 \\ 0 & 0 & g'_{T*}(\vec{q}) \end{pmatrix}^{ab}. \tag{50}$$

For this coordinate system we defined indices $a,b=\{L,T,T^*\}$. We introduce linewidths according to

$$G'_L(\vec{q},\omega)\equiv g'_L(\vec{q},\omega),\quad G'_T(\vec{q},\omega)\coloneqq g'_T(\vec{q},\omega)-i\omega_{\vec{q}}. \tag{51}$$

The column vectors of $T_{\vec{q}}$ are right eigenvectors of M while the row vectors of $T_{\vec{q}}^{-1}$ span the corresponding dual space

$$T_{\vec{q}}^{ia}=:[n_a^i(\vec{q})]^*=\{[\vec{n}_L(\vec{q})\vec{n}_T(\vec{q})\vec{n}_{T^*}(\vec{q})]^*\}^{ia},$$

$$[T_{\vec{q}}^{-1}]^{ai}=:m_a^i(\vec{q})=\begin{bmatrix} \vec{m}_L^T(\vec{q}) \\ \vec{m}_T^T(\vec{q}) \\ \vec{m}_{T*}^T(\vec{q}) \end{bmatrix}^{ai}, \tag{52}$$

$$\vec{m}_a^{\dagger}(\vec{q})\cdot\vec{n}_b(\vec{q})=\delta_{ab}.$$

If $T_{\vec{q}}$ is unitary we have

$$T_{\vec{q}}^{-1}=T_{\vec{q}}^{\dagger},\quad \vec{m}_a(\vec{q})=\vec{n}_a(\vec{q}). \tag{53}$$

Now we get the following representation for the matrix ϕ:

$$\phi(\vec{q},\omega)=i\sqrt{\chi_{\vec{q}}}T_{\vec{q}}[T_{\vec{q}}^{-1}M^{-1}(\vec{q},\omega)T_{\vec{q}}]^{-1}T_{\vec{q}}^{-1}\sqrt{\chi_{\vec{q}}}$$

$$=i(\sqrt{\chi_{\vec{q}}}T_{\vec{q}})\frac{1}{\omega\cdot\mathbf{1}+ig'(\vec{q})}(T_{\vec{q}}^{-1}\sqrt{\chi_{\vec{q}}}), \tag{54}$$

or, equivalently,

$$\phi^{ij}(\vec{q},\omega)=i\sum_{a=\{L,T,T^*\}}\frac{M_a'^{ij}(\vec{q})}{\omega+ig'_a(\vec{q})}, \tag{55}$$

$$M_a'^{ij}(\vec{q})=\sqrt{\chi_{\vec{q}}^i\chi_{\vec{q}}^j}[\vec{n}_a^i(\vec{q})]^*\vec{m}_a^j(\vec{q}). \tag{56}$$

Hence, the relaxation function is a sum of three Lorentzians in the general dipolar case. The tonsorial structure, however, is as yet unspecified. The matrix $T_{\vec{q}}$, which determines the weight factors (56), depends on $\Gamma(\vec{q})$ and either has to be determined self-consistently together with $\Gamma(\vec{q})$ or an additional assumption on the tonsorial structure has to be made. This is different from the isotropic case and generalizes the Lorentzian approximation.

Now, we insert Eq. (55) into Eq. (46) and carry out the frequency integration along the contour shown in Fig. 2.

Defining I'_{ab} by

$$\int_{-\infty}^{\infty}\frac{d\omega'}{2\pi}\phi^{km}(\vec{q}',\omega')\phi^{ln}(\vec{q}-\vec{q}',\omega-\omega')$$

$$=-i\sum_{ab}M_a'^{km}(\vec{q}')M_b'^{ln}(\vec{q}-\vec{q}')$$

$$\times\int_{-\infty}^{\infty}\frac{d\omega'}{2\pi i}\frac{1}{\omega'+ig'_a(\vec{q}')}\frac{1}{\omega-\omega'+ig'_b(\vec{q}-\vec{q}')}$$

$$=:\sum_{ab}M_a'^{km}(\vec{q}')M_b'^{ln}(\vec{q}-\vec{q}')I'_{ab}(\vec{q}',\vec{q}-\vec{q}',\omega), \tag{57}$$

this yields

$$I'_{ab}(\vec{q}',\vec{q}-\vec{q}',\omega)=\frac{i}{\omega+ig'_a(\vec{q}')+ig'_b(\vec{q}-\vec{q}')}. \tag{58}$$

Transforming the damping matrix into the coordinate system

$$G'^{ab}(\vec{q}) := (T_{\vec{q}}^{-1})^{ai}\Gamma^{ij}(\vec{q})T_{\vec{q}}^{jb}, \tag{59}$$

we get

$$G'^{cd}(\vec{q},\omega) = 4k_BT\int_{\vec{q}'}\sum_{ab}\frac{1}{2}T_{cd}^{ab}(\vec{q}',\vec{q}-\vec{q}')\cdot I'_{ab}(\vec{q}',\vec{q}-\vec{q}',\omega), \tag{60}$$

where the kernel T_{cd}^{ab} has been defined as

$$T_{cd}^{ab}(\vec{q}',\vec{q}-\vec{q}') = \sum_{ijkmln}\left\{(T_{\vec{q}}^{-1})^{ci}\frac{1}{\sqrt{\chi_{\vec{q}}^{i}\chi_{\vec{q}}^{j}}}T'_{ijkmln}(\vec{q}',\vec{q}-\vec{q}') \times T_{\vec{q}}^{jd}M_a'^{km}(\vec{q}')M_b'^{ln}(\vec{q}-\vec{q}')\right\}. \tag{61}$$

The final mode-coupling equations for the scaling functions of the damping G_{ab}, which we will solve numerically in the following section, are therefore given in scaling form by

$$G_{cd}(x,y,\vartheta,\nu) = \frac{1}{4}\hat{c}\int\frac{d^3\kappa}{(2\pi)^3}\sum_{ab}\hat{t}_{cd}^{ab}(x,y,\vartheta,\vec{\kappa}) \times\hat{I}'_{ab}(x,y,\vartheta,\vec{\kappa},\nu). \tag{62}$$

Here, the scaling function for the frequency integral has the form

$$\hat{I}'_{ab}(x,y,\vartheta,\vec{\kappa},\nu)^{-1} = -i\nu+\kappa^z g_a\left(\frac{x}{\kappa},\frac{y}{\kappa},\vartheta'\right) + \kappa_-^z g_b\left(\frac{x}{\kappa_-},\frac{y}{\kappa_-},\vartheta''\right), \tag{63}$$

and the kernel can be written as

$$\hat{t}_{cd}^{ab}(x,y,\vartheta,\vec{\kappa}) = \frac{1}{\kappa^2\kappa_-^2}w_c^{ab}(x,y,\vartheta,\vec{\kappa})[\tilde{w}_d^{ab}(x,y,\vartheta,\vec{\kappa})]^*, \tag{64}$$

with

$$w_c^{ab}(x,y,\vartheta,\vec{\kappa}) = (2\kappa\eta-1)\vec{u}_c\cdot\{\vec{w}_a(\vec{\kappa})\times\vec{w}_b(\vec{\kappa}_-)\} + y^2\vec{u}_c\{[\vec{w}_a(\vec{\kappa})\hat{w}(\vec{\kappa})]\cdot[\hat{w}(\vec{\kappa})\times\vec{w}_b(\vec{\kappa}_-)] + [\vec{w}_b(\vec{\kappa}_-)\hat{w}(\vec{\kappa}_-)]\cdot[\hat{w}(\vec{\kappa}_-)\times\vec{w}_a(\vec{\kappa})]\},$$

$$\tilde{w}_d^{ab}(x,y,\vartheta,\vec{\kappa}) = (2\kappa\eta-1)\vec{u}_c^0\cdot\{\vec{w}_a^0(\vec{\kappa})\times\vec{w}_b^0(\vec{\kappa}_-)\} + y^2\vec{u}_c^0\{[\vec{w}_a^0(\vec{\kappa})\hat{w}(\vec{\kappa})]\cdot[\hat{w}(\vec{\kappa})\times\vec{w}_b^0(\vec{\kappa}_-)] + [\vec{w}_b^0(\vec{\kappa}_-)\hat{w}(\vec{\kappa}_-)]\cdot[\hat{w}(\vec{\kappa}_-)\times\vec{w}_a^0(\vec{\kappa})]\}. \tag{65}$$

For clarity we omitted the dependence on the scaling variables x, y, and ϑ of all vectors appearing in these formulas, which are defined by

$$\vec{u}_c(x,y,\vartheta) = \sum_i\frac{m_c^i(\vec{q})}{\sqrt{\chi_{\vec{q}}^i}}\vec{v}_i(\vec{q}),$$

$$\vec{w}_a(x,y,\vartheta,\vec{\kappa}) = \sum_i[n_a^i(\vec{q}')]^*\sqrt{\chi_{\vec{q}'}^i}\vec{v}_i(\vec{q}'),$$

$$\vec{u}_c^0(x,y,\vartheta) = \sum_i\frac{n_c^i(\vec{q})}{\sqrt{\chi_{\vec{q}}^i}}\vec{v}_i(\vec{q}), \tag{66}$$

$$\vec{w}_a^0(x,y,\vartheta,\vec{\kappa}) = \sum_i[m_a^i(\vec{q}')]^*\sqrt{\chi_{\vec{q}'}^i}\vec{v}_i(\vec{q}'),$$

$$\hat{w}(x,y,\vartheta,\vec{\kappa}) = \sum_i\hat{m}^i(\phi,\vartheta')\vec{v}_i(\vec{q}').$$

In the isotropic limit, longitudinal and transverse modes decouple [the damping matrix in Eq. (60) is diagonal] and the longitudinal width is computed at $\omega=0$ while the spin-wave linewidths are evaluated at the spin-wave frequency $\omega=\omega_{\vec{q}}$. This is not possible here, since in general the matrices M_a' do not commute and the corresponding modes cannot be decoupled. Thus, to remain consistent we evaluate all damping constants at zero frequency as in the paramagnetic case. This is equivalent to the assumption that the frequency-dependent damping coefficients vary slowly even on the scale of the spin-wave frequency and not only on the scale of the linewidths. In the isotropic case,[11] the longitudinal linewidth always exceeds the spin-wave frequency. Later we will see that this property also holds in the dipolar case. Thus, this assumption is not more restrictive than in the isotropic case. A consequence of this choice are the following very useful symmetry properties:

$$[G_{cd}(x,y,\vartheta)]^* = G_{c^*d^*}(x,y,\vartheta),$$

$$[w_c^{ab}(x,y,\vartheta,\vec{\kappa})]^* = w_{c^*}^{a^*b^*}(x,y,\vartheta,\vec{\kappa}), \tag{67}$$

which derive from $G_{ij}(\nu=0)\in\mathbb{R}$ and where we defined the index mapping

$$L^* := L, \quad (T)^* := T^*, \quad (T^*)^* := T. \tag{68}$$

Finally, we have to determine the diagonalizing matrix $T_{\vec{q}}$ entering Eq. (50). If one prefers a self-consistent determination together with the damping matrix, it is advantageous to eliminate $T_{\vec{q}}$ from the equations. This leads to double matrices (objects with four indices) and the corresponding expressions are given in Appendix C. Here, we introduce a simplifying assumption about $T_{\vec{q}}$. This has the advantage that we can start with a fixed $T_{\vec{q}}$ from the beginning. Due to the reduced symmetry of the problem the Lorentzian approximation not only requires assumptions about the linewidths as in the isotropic case but also about the tensor structure.

There are four complementary limiting cases where $T_{\vec{q}}$ can be determined in advance. They are described in detail in Appendix D. For all these cases, the result can be written as

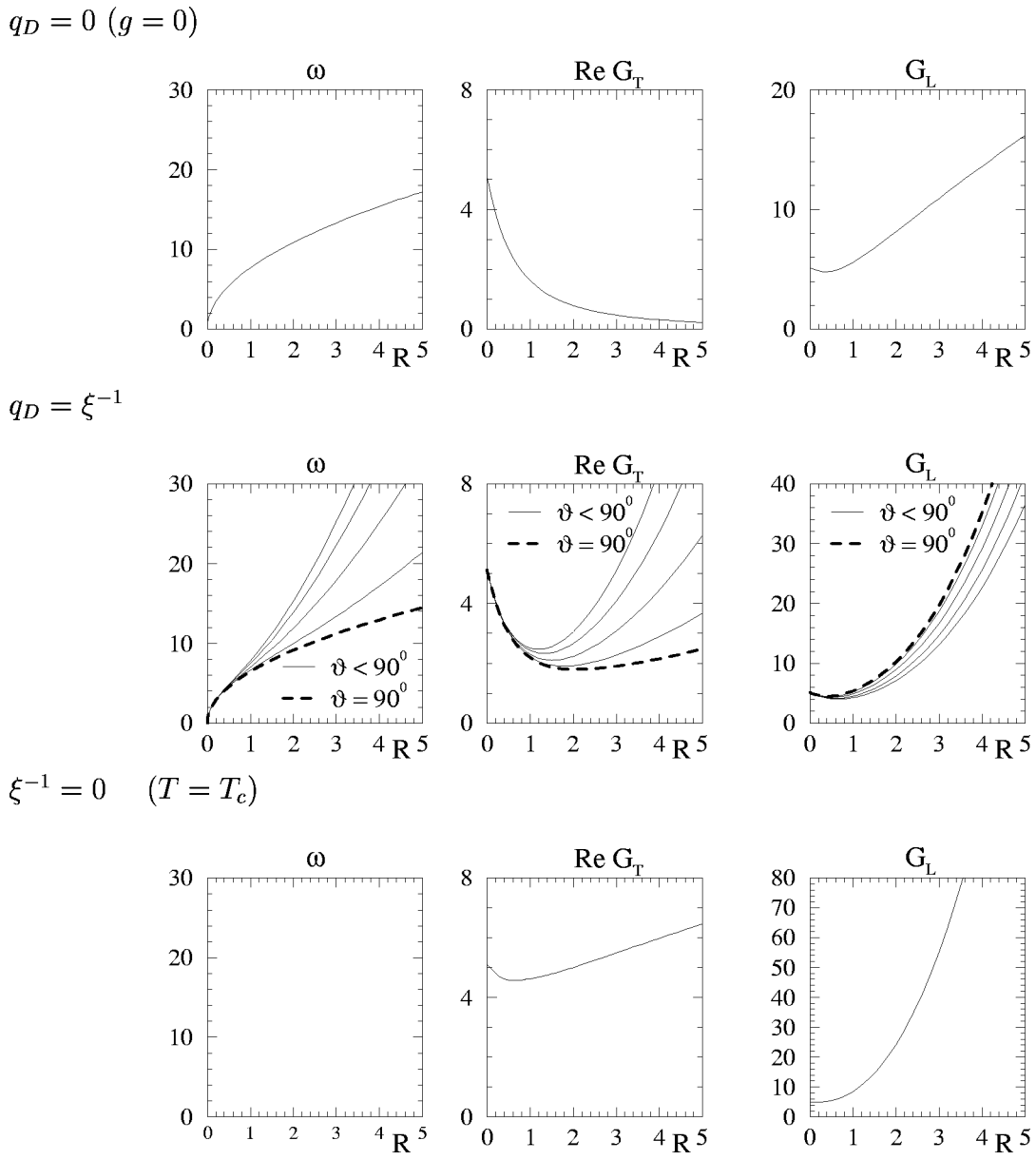

FIG. 3. Scaling functions for the spin-wave frequency, the transverse and the longitudinal linewidth vs R for various values of ϑ ($\vartheta = 18°i$, $i = 1,\ldots,5$) for the isotropic limit (uppermost row), a typical dipolar case (here $\phi = 45°$, i.e., $\xi^{-1} = q_D$, middle row), and at T_c (bottom row).

$$T_{\vec{q}} = \begin{pmatrix} 0 & \frac{1}{\sqrt{2}} & \frac{1}{\sqrt{2}} \\ 0 & -\frac{i}{\sqrt{2}} & \frac{i}{\sqrt{2}} \\ -1 & 0 & 0 \end{pmatrix}. \tag{69}$$

Therefore, we use this expression also in the general case. There is a second justification of this choice of $T_{\vec{q}}$: Because it amounts to using the static eigenvectors as a basis also for the dynamics, the most significant geometric effects of the dipolar interaction, which determine the directions of the eigenvectors, are already incorporated. For example, the change of the direction of the longitudinal mode from the direction of the magnetization in the isotropic case to the direction of the wave vector at T_c is automatically included. Thirdly and finally, the validity can be scrutinized by evaluating the off diagonal elements of G_{ab} *a posteriori*. We found that they are indeed small in the four indicated regions (Appendix D) and near the line $x \approx y$. For larger values of R there are deviations from the assumed diagonality. But since the results at large R do not influence the results at small R significantly in our self-consistent solution, we conclude that our results should be correct for the values of R, which are relevant for the comparison with experiment ($R \lesssim 5$).

VI. NUMERICAL SOLUTION AND RESULTS

Before we come to the results of our calculations, we briefly describe the numerical procedure for the solution of our coupled integral equations, the mode-coupling equations (62). The integrand functions depend on the quantities to be determined through the scaling functions $\hat{I}'_{ab}$ in Eq. (62) and

therefore, we utilize an iterative method to solve this self-consistency problem. We take starting values for G_{cd}, then calculate a set of functions via Eqs. (62), and iterate until convergence is achieved. Due to the characteristic structure of the equations (the function to be determined enters the denominator of the right-hand side which has to be integrated over), there is a tendency to smooth out any deviations from the true solution and the procedure converges. Furthermore, it has been shown that under certain circumstances the solution of such mode-coupling equations is unique and if the procedure converges at all, then it converges uniquely to one solution.[60] The key ingredient is the three-dimensional integration in wave-vector space. Since almost all symmetries are lost in our case, and since the functions depend on so many variables, a very fast integration procedure is indispensable. The time necessary for one iteration increases approximately by a factor of 200 compared with the isotropic case. We have therefore chosen to employ Gaussian quadrature rules with a nonadaptive fixed integration mesh. Rather, it has been optimized in advance to best integrate the specific integrands we deal with. This was possible, because the main features of the integrand functions are determined by the known kernels (65). For the highest accuracy we used 16 000 mesh points for the integration, which was carried out at each of the 7400 mesh points for the external scaling variables. This iteration step was repeated about 10 to 20 times. The relative error of the functions is estimated to be less than 10^{-2}.

The result of the mode-coupling equations (62) are then the scaling functions for the linewidths. The linewidths are the eigenvalues of the matrix (59) assumed to be diagonal in the reference frame of the static eigenvectors (cf. the discussion at the end of Sec. V). When speaking of a longitudinal line width we therefore mean the linewidth of magnetization fluctuations in the direction of the eigenvector $\vec{v}_3$ of the static susceptibility. It is real and depends on the two scaling variables R and ϕ, and the angle ϑ characterizing the direction of the wave vector $\vec{q}$ relative to the magnetization $\vec{M}$. The transverse line width is complex where the real part determines the actual linewidth while the imaginary part leads to a frequency shift which alters the spin-wave frequency. This imaginary part is, however, very small and the spin-wave frequency is still approximately given by Eq. (27). This is quite analogous to the isotropic case, where the correction to the excitation energies was also on the order of a few per cent only. The only exception occurs very close to T_c where the spin-wave energy vanishes and the relative deviation therefrom can become larger.[11] The spin-wave frequency has already been discussed in Sec. IV. We have drawn the corresponding scaling functions in the left column of Fig. 3 for various values of the scaling variable ϕ. They have been calculated using the value $\hat{b}=7.7$ for the amplitude of the spin-wave frequency. Using $G_L(R=0)=G_T(R=0)=5.13$, i.e., using $\hat{c}=8\pi^4$, this corresponds to $W_-=\hat{b}/G(0)=1.5$. (For a detailed discussion of the universal amplitude $\hat{b}$ and W_- see Refs. 58 and 59.) In the bottom row, at $\phi=90°$, which is equivalent to $T=T_c$, the spin-wave frequency vanishes.

The damping of the spin waves is shown in the middle column of Fig. 3. Comparing the uppermost row, which corresponds to the isotropic case, with the other rows we see that the damping is increased due to the dipolar interaction. This is not unexpected, since the magnetization is no longer conserved in the presence of the dipolar interaction. The corresponding lifetime decreases and the linewidth is increased. Furthermore, we see a strong dependence on the angle ϑ. The damping is largest when the direction of $\vec{q}$ characterizing the dipolar interaction lies completely in the plane of the transverse modes ($\vartheta=0°$), perpendicular to the magnetization. The most prominent feature is certainly the minimum in the scaling function, which is in very marked contrast to the monotonic decrease in the pure isotropic case.

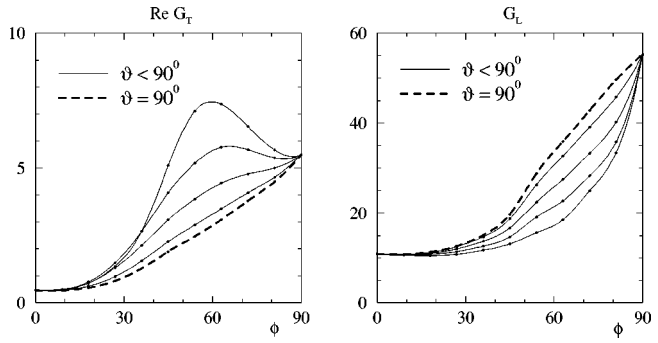

FIG. 4. Variation of $\Re G_T$ and G_L with ϕ for various values of ϑ ($\vartheta=18°\,i$, $i=1,\ldots,5$) for $R=3$.

If we take a closer look at the variation with ϕ, i.e., with temperature or with increasing dipolar influence, we see in the left part of Fig. 4, that the increase is not always monotonic but rather has a maximum as a function of ϕ if ϑ is sufficiently small. This is very similar to the paramagnetic dipolar case where the variation of the transverse linewidth also showed a maximum as a function of ϕ.[11]

In the right column of Fig. 3 the longitudinal linewidths are drawn. These, too are larger than in the isotropic case for the same reason. The variation with the angle ϑ is less pronounced here and the linewidth is largest when the wave vector $\vec{q}$ is parallel to $\vec{M}$ ($\vartheta=90°$). Since the dipolar interaction is characterized by the direction of the wave vector $\vec{q}$, and the longitudinal mode is characterized by the direction of the spontaneous magnetization $\vec{M}$, this means that again, as for the transversal excitations, the damping is largest, when the direction characterizing the dipolar interaction is parallel to the direction characterizing the corresponding mode, which is the longitudinal mode this time. For small values of R (for $q>q_D$), the scaling function is approximately constant, the corresponding linewidth shows critical $q^{5/2}$ behavior. For smaller q, however, the scaling function grows as $R^{5/2}$, which means that the linewidth itself becomes constant. This exactly parallels the situation above T_c. Due to the nonconservation of the magnetization this mode becomes uncritical. Therefore, the kinetic coefficient is finite, as in the classical van Hove scenario. Since also the static longitudinal susceptibility eventually is constant in the dipolar case,[21] the quotient, i.e., the damping, is constant in the limit $q\to 0$. Also the variation of G_L with ϕ (see right part of Fig. 4) is similar to the paramagnetic dipolar case, since it shows a monotonic increase.[11] It is important to note, that the longitudinal linewidth is still larger or of the same size as the spin-wave frequency as in the isotropic case. First, this gives

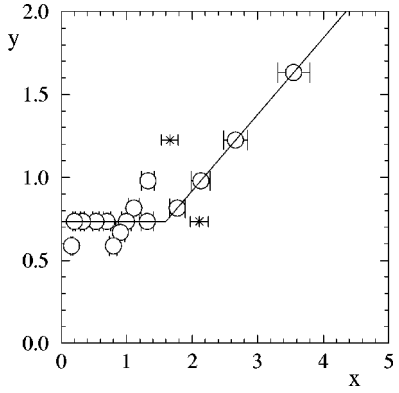

FIG. 5. Distribution of the measurements from Ref. 61 for EuO in the x-y plane. See text for details.

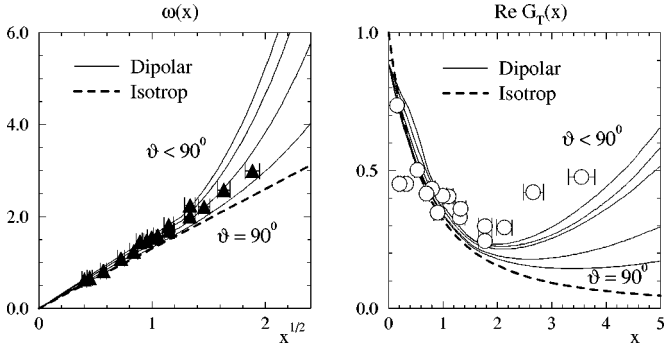

FIG. 6. Left: Scaling function of spin-wave frequency vs scaling variable $x^{1/2}$. Theoretical curves are for $\vartheta = 18° i$, $i = 1,\ldots,5$, experimental points are for EuO (from Ref. 61). Dashed: Scaling function in the isotropic limit. Right: Same for the scaling function of the transverse linewidth vs x.

an *a posteriori* justification of our assumption that the approximation of slowly varying damping on the scale of the spin-wave frequency is not more restrictive than a slow variation on the scale of the dampings. (See the discussion in Sec. V.) Secondly, it implies that experimentally it is necessary to use polarized neutrons in order to detect the longitudinal peak, since by using unpolarized neutrons the longitudinal peak would be masked by the spin-wave peaks.

VII. COMPARISON WITH EXPERIMENT

In this final section we want to compare our findings with two experiments. The first was performed on EuO by Passell *et al.*[61] measuring spin-wave frequencies and the corresponding linewidths at a variety of temperatures and wave vectors. Due to the availability of unpolarized neutrons only, they were not able to detect the longitudinal peak and hence could not determine the longitudinal damping. Each measurement at a specific temperature and wave vector corresponds to a point in the plane of the scaling variables x and y. These points are shown in Fig. 5.

The error bars in the x direction correspond to the uncertainty in the correlation length. In Ref. 61 the experiments were compared with the isotropic model, which corresponds to a comparison between the measurements and the theoretically determined function taken on the x axis ($y=0$) in Fig. 5. Here, we made a comparison between the experiment and the theoretical scaling functions along the trajectory plotted in Fig. 5. Since the separation of the two measured points marked with a star from this trajectory is too large, we omitted them in the comparison. In Fig. 6 we plot the corresponding scaling functions vs the scaling variable $x^{1/2}$ and x, respectively. Note that we plot the total spin-wave energy, which can be obtained from the exchange spin-wave energy given in Ref. 61 by the following transformation:

$$E_{\mathrm{tot}} = E_{\mathrm{ex}} f(q), \tag{70}$$

where the factor $f(q)$ is given by $f(q) = 1/2 + [(1+\phi)/2/\sqrt{\phi}]\arctan\sqrt{\phi}$, $\phi = 0.024\ \text{Å}^{-2} q^{-2}$ [see formula (33) in Ref. 61]. When plotted vs $x^{1/2}$, the isotropic limit yields a straight line through the origin.

Figure 6 shows the possible range of the theoretical curves when varying the angle ϑ. Since the sample was a polycrystalline powder, the angle between the wave vector and the magnetization is not sharply defined, and the actual theoretical prediction would be a weighted average over the curves shown in the figure. To obtain the scaling functions experimentally one has to divide by the critical damping at T_c. Both experimental and theoretical linewidths are then normalized to 1 at $x = y = 0$. The damping could well be parametrized by the formula $\Gamma_q = A' q^{5/2} f(q)$. The value of the amplitude A' measured in Ref. 61, however, seems to suffer from experimental uncertainties. In later measurements[62,63] and also in very recent measurements[64] the values are roughly a factor of 1.5 bigger than the value $A' = 4.0$ meV Å$^{2.5}$ found in Ref. 61. We have therefore chosen the value $A' = 6.60$ meV Å$^{2.5}$. At $q = 0.15$ Å^{-1} we have $f(q) \approx 1.30$ and thus $A \approx A' f(q) \approx 8.58$ meV Å$^{2.5}$ (cf. Refs. 58, 59). This yields for the universal amplitude of the spin-wave frequency scaling function a value $W_- = 1.3$ or $\hat{b} = 6.7$ (cf. Refs. 58, 59). This is the value used for the theoretical curves in Fig. 6. Note that we have used no fit parameter.

As can be seen from the figure, especially the data for the damping are by far better represented by the dipolar curves, which show a minimum, than by the isotropic curve, which exhibits a monotonic decrease (dashed curve in Fig. 6). The isotropic theory cannot even qualitatively explain the measurements.

The second experiment we want to discuss is a recent experiment on Ni by Böni *et al.*,[1,65] who used polarized neutrons and thus could clearly identify the longitudinal peak. They performed their measurements in a restricted temperature region (values of ϕ lie between 26° and 30°) such that we can compare the data with theoretical curves for $\phi = 28°$. The scatter in the data for the scaling function of the longitudinal linewidth (Fig. 7) is quite large, but since the scaling function is normalized to unity at $x = y = 0$ and on the other hand has to increase as $x^{5/2}$ (the damping itself becomes constant in the asymptotic dipolar regime for $q \to 0$), the data give clear evidence for a minimum.

In Refs. 58, 59 it is shown, that the numerical value of the universal amplitude of the spin-wave frequency $\hat{b}$ is crucial for obtaining a minimum in the scaling function. There, it is also shown, that such a minimum already occurs in the isotropic theory, provided the right value for $\hat{b}$. Here, we show that also in the dipolar theory the experimental results are in agreement with theory. Obviously the deviations from the isotropic theory are not yet very pronounced in the region of

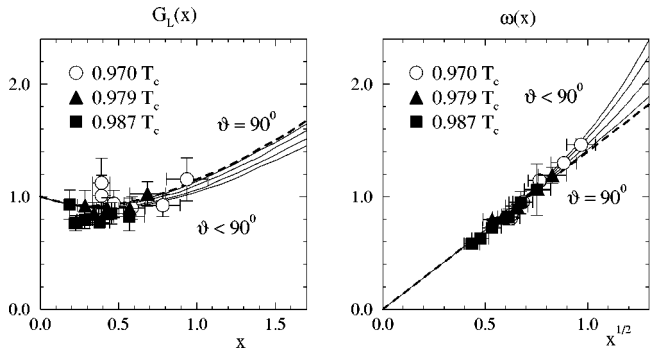

FIG. 7. Left: Scaling function of longitudinal linewidth and data points from Refs. 1, 65 for Ni vs scaling variable x. Right: Scaling function of the corresponding spin-wave frequency for various angles ϑ ($\vartheta = 18°i$, $i = 1,\ldots,5$) vs $\sqrt{x}$.

the comparably small x probed in the experiment, where no strong dipolar effects are expected. Furthermore the dipolar interaction in Ni is only weak, since the dipolar wave vector is small. Farther away from T_c or alternatively at smaller wave vectors the dipolar influences should be noticeable. The value of the spin-wave amplitude can be determined by independent experiments and we have taken $W_- = 1.4$ or equivalently $\hat{b} = 7.2$. Then, there seems to be a slight indication for a deviation of the frequency data from the isotropic prediction—a straight line through the origin when plotted vs $\sqrt{x}$. The dipolar dispersion fits the data better, but the fairly large error bars prevent a decisive conclusion. Note that there are no fit parameters available.

VIII. SUMMARY AND CONCLUSIONS

In this paper we have shown that the dipolar interaction drastically affects the critical dynamics of Heisenberg ferromagnets below T_c. We derived and solved self-consistently mode-coupling equations for the temperature and wave-vector dependence of the linewidths for this model, which take full account of the complicated tonsorial structure of the problem.

This also results in a very intricate mode structure, which can be summarized as follows. For the static properties, the longitudinal direction is defined along the eigenvector $\vec{v}_1$ of the static susceptibility tensor χ associated with the longitudinal susceptibility (which is defined as the smallest or least divergent of the three eigenvalues or susceptibilities). It lies in the plane spanned by the wave vector $\vec{q}$ and the magnetization $\vec{M}$. The two transverse directions are defined as the two remaining eigenvectors $\vec{v}_2$ and $\vec{v}_3$. They are mutually perpendicular to one another and perpendicular to the longitudinal direction.

Although the susceptibility tensor χ and the frequency matrix ω cannot be diagonalized simultaneously, approximately the dynamic eigendirections coincide with the static. Therefore, the longitudinal direction $\vec{v}_1$ also defines the direction of the longitudinal spin-relaxation mode, while the two transverse directions $\vec{v}_2$ and $\vec{v}_3$ span the plane of the two spin-wave modes. Thereby, the complicated crossover from the isotropic limiting case (the longitudinal mode is along the magnetization $\vec{M}$) to the dipolar limiting case at T_c (there is no spontaneous magnetization and the longitudinal mode is along the wave vector $\vec{q}$) is described consistently.

In our calculations we limited ourselves to a generalization of the Lorentzian approximation. In Sec. V, we introduced a general derivation of a Lorentzian approximation, based on the assumption that the damping coefficients entering the relaxation function can be considered frequency independent. In the general case, the matrix character of these quantities cannot be neglected. The (tensorial) relaxation function is a sum of three Lorentzians, where the sum is weighted with some (tensorial) weights.

We have found that the dipolar interaction not only modifies the static susceptibilities markedly, but also the spin-wave frequency and the linewidths of the excitations are altered. The spin-wave frequency $\omega_{\vec{q}}$ is increased, which can be described by a pseudogap for larger values of the wave vector (cf. Fig. 1). This enhancement depends on the angle between the magnetization $\vec{M}$ and the wave vector $\vec{q}$. The largest deviations from isotropic behavior occur when $\vec{q}$ is perpendicular to $\vec{M}$, i.e., when $\vec{q}$ lies completely in the plane of the transverse modes, perpendicular to the longitudinal mode. For small q, the dispersion is modified from quadratic to linear in q (cf. Fig. 1). This directly corresponds to the disappearance of one Goldstone mode in the general dipolar case. An indication for this behavior can be found in experiments on EuO and Ni (cf. Fig. 6, left, and Fig. 7, right). Our expression for the spin-wave frequency agrees with spin-wave theory in the common range of validity.

The associated transverse damping is also increased compared to the isotropic case with a similar angular dependence. Most significant is a minimum in the transverse scaling functions as compared to the monotonic decrease in the isotropic limit (cf. top row vs middle row in Fig. 3). This also compares favorably with experiments conducted on EuO (cf. Fig. 6, right). The frequency shift described by an imaginary part of the damping is small. This parallels the situation above T_c. The temperature variation (we found a maximum when varying the scaling variable ϕ, cf. Fig. 4, left) is also similar to the paramagnetic case. However, the height of the maximum depends on the angle ϑ between $\vec{q}$ and $\vec{M}$ and gets smaller, the more the wave vector $\vec{q}$ gets parallel to the magnetization $\vec{M}$.

The longitudinal damping G_L' is also increased compared to the isotropic value. It is largest when the wave vector is parallel to $\vec{M}$, i.e., when $\vec{q}$ lies in the associated longitudinal direction (cf. middle row of Fig. 3). At $q \approx q_D$, we find a crossover from the critical $q^{5/2}$ asymptotics to a noncritical q^0. Furthermore, the variation with ϕ again is monotonic (cf. Fig. 4, right). The dependence on the angle ϑ is less pronounced than for the transverse damping. Since $G_L' \gtrsim \omega_{\vec{q}}$, the corresponding broad central peak can be detected experimentally only by means of polarized neutrons as in the isotropic limit, i.e., polarized neutrons will be necessary to resolve the complete peak structure.

ACKNOWLEDGMENTS

It is a pleasure to thank U. C. Täuber and E. Frey for valuable and helpful discussions. The authors would like to

thank P. Böni for providing them with the numerical values of the measurements from Ref. 1 and for some valuable discussions. Also, discussions with S. Schorr and C. Pich are gratefully acknowledged. This work was supported by the German Federal Ministry for Research and Technology (BMFT) under Contract Nos. 03-SC3TUM and 03-SC4TUM2.

APPENDIX A: STATIC SUSCEPTIBILITIES

The susceptibilities $\chi^i_{\vec{q}} = 1/2Jq^2 l_i$, $(i=1,2,3)$, which are the eigenvalues of the susceptibility tensor, are given by

$$l_1(R,\phi,\vartheta)=1, \quad l_{2/3}(R,\phi,\vartheta)=1+\tilde{R}^2\hat{F}_{\mp}(\vartheta,\phi),$$

$$\hat{F}_{\pm}(\vartheta,\phi)=\frac{1}{2}\{1\pm\sqrt{1-\sin^2 2\tilde{\phi}\,\cos^2\vartheta}\},$$

$$\tilde{R}(R,\phi)=\sqrt{\hat{r}^2(x,y)+y^2}, \quad \tan\tilde{\phi}(R,\phi)=y/\hat{r}(x,y). \tag{A1}$$

Here, we used a mass function[21]

$$\hat{r}^2(x,y)=\frac{29x^2}{18+2x[1+(1+y^2)^{-1/2}]} - \frac{9x^2}{11}\left[1+\sqrt{1+4x^2}\,\ln\left(\frac{\sqrt{1+4x^2}-1}{2x}\right)\right]+O(\varepsilon^2), \tag{A2}$$

and already introduced scaling variables. The fact that the scaling functions depend on two scaling variables instead of only one is called generalized scaling law and is a direct consequence of the dipolar interaction as outlined in the Introduction. The angle ϑ precisely[21] is defined together with the unit vector $\hat{p}$ according to

$$\vec{q}=:q\,\mathrm{sgn}\,\vec{q}\begin{pmatrix}\cos\varphi\,\cos\vartheta\\ \sin\varphi\,\cos\vartheta\\ \sin\vartheta\end{pmatrix}, \tag{A3}$$

$$\hat{p}:=\begin{pmatrix}\cos\varphi\\ \sin\varphi\\ 0\end{pmatrix}:=\begin{cases}\dfrac{\vec{e}_z\times(\vec{q}\times\vec{e}_z)}{p}\,\mathrm{sgn}\,\vec{q} & \text{for } p:=\sqrt{q_x^2+q_y^2}\neq 0,\\ \vec{e}_y & \text{for } p=0,\end{cases} \tag{A4}$$

$$\mathrm{sgn}\,\vec{q}:=\begin{cases}\mathrm{sgn}\,q_z, & q_z\neq 0,\\ \mathrm{sgn}\,q_y, & q_z=0, \quad q_y\neq 0,\\ \mathrm{sgn}\,q_x, & q_z=q_y=0, \quad q_x\neq 0,\\ 1, & q=0.\end{cases} \tag{A5}$$

The eigenvectors are then defined through

$$\vec{v}_1(\vartheta,\phi)=\hat{p}\times\hat{e}_z,$$

$$\vec{v}_{2/3}(\vartheta,\phi)=\cos\varphi_{2/3}(\vartheta,\phi)\hat{p}+\sin\varphi_{2/3}(\vartheta,\phi)\hat{e}_z, \tag{A6}$$

$$\varphi_3(\vartheta,\phi)=\varphi_2(\vartheta,\phi)+90^\circ=\frac{1}{2}\arccos f(\vartheta,\phi)\in[0^\circ,90^\circ],$$

$$f(\vartheta,\phi)=\frac{\sin^2\tilde{\phi}\,\cos 2\vartheta-\cos^2\tilde{\phi}}{\sqrt{1-\sin^2 2\tilde{\phi}\,\cos^2\vartheta}}, \quad f(0^\circ,45^\circ):=-1.$$

This is a right handed orthogonal coordinate system. Instead of the Cartesian coordinate system we therefore use the coordinate system introduced in the previous paper (see Fig. 1 of Ref. 21). One direction ($\vec{v}_1$) is perpendicular to the wave vector $\vec{q}$ and the magnetization $\vec{M}$, while the other two directions ($\vec{v}_2$ and $\vec{v}_3$, perpendicular to each other) lie in the $\vec{q}$-$\vec{M}$ plane. Their orientation relative to $\vec{q}$ and $\vec{M}$ is rather complicated, however, and we refer the reader to Ref. 21 for details.

Instead, we introduce some more scaling variables. If we define

$$\vec{q}'':=\vec{q}-\vec{q}'=q\cdot\vec{\kappa}_-, \tag{A7}$$

the polar coordinates $\kappa_-,\vartheta'',\varphi''$ of $\vec{\kappa}_-$ are given by

$$\kappa_-^2=1+\kappa^2-2\kappa\eta,$$

$$\eta=\frac{\vec{q}\vec{q}'}{qq'}=\cos(\varphi'-\varphi_{\vec{q}})\sin\vartheta_{\vec{q}}\,\sin\vartheta'+\cos\vartheta_{\vec{q}}\,\cos\vartheta',$$

$$\cos\vartheta''=\frac{\cos\vartheta_{\vec{q}}-\kappa\,\cos\vartheta'}{\kappa_-},$$

$$\sin\vartheta''=\frac{\sqrt{\sin^2\vartheta_{\vec{q}}+\kappa^2\sin^2\vartheta'-2\kappa\cos(\varphi'-\varphi_{\vec{q}})\sin\vartheta_{\vec{q}}\sin\vartheta'}}{\kappa_-},$$

$$\cos(\varphi''-\varphi_{\vec{q}})=\frac{\sin\vartheta_{\vec{q}}-\kappa\,\cos(\varphi'-\varphi_{\vec{q}})\sin\vartheta'}{\kappa_-\,\sin\vartheta''},$$

$$\sin(\varphi''-\varphi_{\vec{q}})=\frac{-\kappa\,\sin(\varphi'-\varphi_{\vec{q}})\sin\vartheta'}{\kappa_-\,\sin\vartheta''}. \tag{A8}$$

In these relations only the relative azimuth angles $\Delta\varphi'=\varphi'-\varphi_{\vec{q}}$ and $\Delta\varphi''=\varphi''-\varphi_{\vec{q}}$ enter.

APPENDIX B: FREQUENCY MATRIX

For the evaluation of the frequency matrix one starts from the commutation rules

$$[S_r^\alpha,S_s^\beta]=i\,\delta_{rs}\varepsilon_{\alpha\beta\gamma}S_r^\gamma \tag{B1}$$

in direct space with lattice points r and s, which in Fourier space read

$$[S_{\vec{q}}^\alpha,S_{\vec{q}'}^\beta]=i\varepsilon_{\alpha\beta\gamma}S_{\vec{q}+\vec{q}'}^\gamma. \tag{B2}$$

Inserting

$$\langle S_{\vec{q}}^{\alpha}\rangle =: \delta_{\vec{q},0}\delta_{\alpha,z}\cdot m \tag{B3}$$

for the thermal expectation value (with the magnetization m), we get the final form of the frequency matrix

$$C_{\vec{q}}^{ij} = i\omega_{\vec{q}}\begin{pmatrix} 0 & \sin\gamma & \cos\gamma \\ -\sin\gamma & 0 & 0 \\ -\cos\gamma & 0 & 0 \end{pmatrix}. \tag{B4}$$

There, the angle γ is defined through static quantities (A1) and (A6):

$$\tan\gamma(R,\phi,\vartheta) = \tan\varphi_3(\phi,\vartheta)\ \sqrt{\frac{l_2(R,\phi,\vartheta)}{l_3(R,\phi,\vartheta)}},$$

$$\gamma\in[0°,90°] \tag{B5}$$

and the spin-wave frequency is given by

$$\omega_{\vec{q}} = 2Jm\sqrt{q^2(q^2+q_D^2\cos^2\vartheta)}. \tag{B6}$$

The eigenvalues of the matrix (B4) are $c_{\vec{q}}^{1}=0$ (connected with the longitudinal mode) and $c_{\vec{q}}^{2/3}=\pm\omega_{\vec{q}}$ (connected with the two transverse spin-wave modes). The corresponding eigenvectors are given by

$$\vec{\omega}^{1} = \vec{a}_z$$

and

$$\vec{\omega}^{2/3} = \vec{a}_{\pm} := \frac{1}{\sqrt{2}}\{\vec{a}_{\perp} \mp i\vec{a}_{\parallel}\}. \tag{B7}$$

Here, we defined

$$\vec{a}_z := -\sin\theta\hat{p} + \cos\theta\hat{e}_z,$$

$$\vec{a}_{\perp} := \hat{p}\times\hat{e}_z,$$

$$\vec{a}_{\parallel} := \cos\theta\hat{p} + \sin\theta\hat{e}_z,$$

$$\theta := \varphi_3 - \gamma. \tag{B8}$$

The vectors $\{\vec{a}_z,\vec{a}_{\perp},\vec{a}_{\parallel}\}$ form a right handed orthogonal coordinate system. The angle $90°-\gamma$ is the angle by which the eigenvectors of the frequency matrix differ from the eigenvectors of the static susceptibility tensor. This is depicted in Fig. 8.

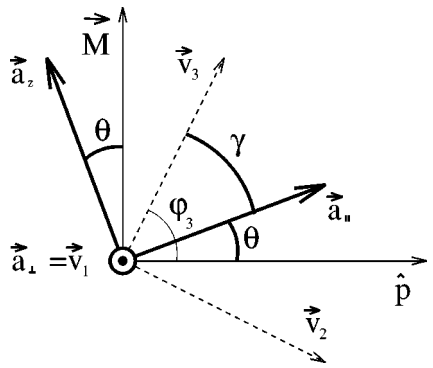

FIG. 8. The eigenvectors of the frequency matrix $\vec{a}_{\perp}$, $\vec{a}_{\parallel}$, and $\vec{a}_z$, and the eigenvectors of the static susceptibility $\vec{v}_i$. The vectors $\vec{a}_{\parallel}$, $\vec{a}_z$, $\vec{v}_2$, and $\vec{v}_3$ lie in the q-M plane, the vectors $\vec{a}_{\perp}$ and $\vec{v}_1$ are perpendicular to that plane. The q-M plane is spanned by $\hat{p}$ and $\vec{M}$, where $\hat{p}$ is the projection of $\vec{q}$ onto the plane perpendicular to $\vec{M}$, normalized to unit length.

$$\phi^{km}(\vec{q}',\omega') = i\sqrt{\chi_{\vec{q}'}^{k}\chi_{\vec{q}'}^{m}}\left[\frac{1}{\omega'\mathbf{1}+ig'(\vec{q}')}\right]^{km}$$

$$= i\sqrt{\chi_{\vec{q}'}^{k}\chi_{\vec{q}'}^{m}}\sum_{a} T_{\vec{q}'}^{ka}\frac{1}{\omega'+ig_a'(\vec{q}')}[T_{\vec{q}'}^{-1}]^{am}. \tag{C1}$$

The matrix elements $[g']^{km}$ are known while the eigenvalues $[g']^{ab}=g_a'\delta_{ab}$ which are needed for the frequency integration are unknown. Performing this integration according to Eq. (57) now yields

$$\int_{-\infty}^{\infty}\frac{d\omega'}{2\pi}\,\phi^{km}(\vec{q}',\omega')\phi^{ln}(\vec{q}-\vec{q}',\omega-\omega')$$

$$= i\sqrt{\chi_{\vec{q}'}^{k}\chi_{\vec{q}'}^{m}\chi_{\vec{q}-\vec{q}'}^{l}\chi_{\vec{q}-\vec{q}'}^{n}}\sum_{ab} T_{\vec{q}'}^{ka}T_{\vec{q}-\vec{q}'}^{lb}$$

$$\times\frac{1}{\omega+ig_a'(\vec{q}')+ig_b'(\vec{q}-\vec{q}')}[T_{\vec{q}'}^{-1}]^{am}[T_{\vec{q}-\vec{q}'}^{-1}]^{bn}. \tag{C2}$$

Obviously, the double sum can be interpreted as a double back transformation of a diagonal matrix which will yield a ''double matrix'' with indices k,m,l,n. After this back transformation the matrix $T_{\vec{q}}$ will have disappeared and we only have to deal with matrix elements of $g'(\vec{q}')$ and $g'(\vec{q}-\vec{q}')$.

To obtain this double matrix we first note that the function of a matrix M can be defined through the function of its eigenvalues λ_i. Let T be the transformation which diagonalizes M:

$$T^{-1}MT = \mathrm{diag}[\{\lambda_i\}] \Leftrightarrow M = T\ \mathrm{diag}[\{\lambda_i\}]T^{-1}. \tag{C3}$$

Then, by using the function f of the eigenvalue, we define

$$f(M) := T\ \mathrm{diag}[\{f(\lambda_i)\}]T^{-1}, \tag{C4}$$

which is itself a matrix. Quite analogous a function of two variables or two eigenvalues transforms into a double matrix.

APPENDIX C: DOUBLE MATRICES

In this appendix we briefly outline the possibility to eliminate the transformation matrix $T_{\vec{q}}$ which diagonalizes M, Eq. (49), from the equations. We start with the representation

We will transform Eq. (C2) in two steps. First we can write

$$\sum_a T^{ka}_{\vec{q}'} \frac{1}{\omega + ig'_a(\vec{q}') + ig'_b(\vec{q}-\vec{q}')} [T^{-1}_{\vec{q}'}]^{am} = \left[\frac{1}{\omega \mathbf{1} + ig'(\vec{q}') + ig'_b(\vec{q}-\vec{q}')\cdot \mathbf{1}} \right]^{km} =: f_{km}[g'(\vec{q}'), \omega + ig'_b(\vec{q}-\vec{q}')]. \quad \text{(C5)}$$

The functions f_{km} need a matrix A and a scalar x as input and are basically the matrix elements of the inverse matrix. Therefore they can be written in the form (for 3×3 matrices)

$$f_{km}(A,x) = \frac{a_{km}x^2 + b_{km}x + c_{km}}{x^3 + dx^2 + ex + f}, \quad \text{(C6)}$$

where the coefficients a_{km}, b_{km}, c_{km}, d, e, and f can be calculated from the matrix elements of A. They can be given in explicit form if one uses a representation of the inverse of a matrix A in terms of a polynomial in A. Let $\tilde{A}$ be defined through

$$\tilde{A} = A^2 - \mathrm{Sp}A \cdot A + \frac{1}{2}[(\mathrm{Sp}A)^2 - \mathrm{Sp}(A^2)]\cdot \mathbf{1}. \quad \text{(C7)}$$

Then, the inverse of A is given by

$$A^{-1} = \frac{\tilde{A}}{\det A} \quad \text{(C8)}$$

for 3×3 matrices and if $\det A \neq 0$. Correspondingly, the coefficients for the calculation of f_{km}

$$f_{km}(A,x) = [f(A,x)]^{km} = \left(\frac{1}{x\mathbf{1} + iA} \right)^{km} = \left[\frac{x^2 \cdot \mathbf{1} + ix(\mathrm{Sp}A \cdot \mathbf{1} - A) - \tilde{A}}{x^3 + i\,\mathrm{Sp}A \cdot x^2 - \mathrm{Sp}\tilde{A} \cdot x - i\ \det A} \right]^{km} \quad \text{(C9)}$$

are given by

$$a_{km} = \delta_{km}, \quad b_{km} = i\,\mathrm{Sp}A\,\delta_{km} - iA^{km}, \quad c_{km} = -\tilde{A}^{km},$$
$$d = i\,\mathrm{Sp}A, \quad e = -\,\mathrm{Sp}\tilde{A}, \quad f = -i\ \det A. \quad \text{(C10)}$$

The second step consists in writing

$$\sum_b T^{lb}_{\vec{q}-\vec{q}'} f_{km}[g'(\vec{q}'), \omega + ig'_b(\vec{q}-\vec{q}')][T^{-1}_{\vec{q}-\vec{q}'}]^{bn} = \{f_{km}[g'(\vec{q}'), \omega\mathbf{1} + ig'(\vec{q}-\vec{q}')]\}^{ln}. \quad \text{(C11)}$$

In doing so we have transformed the matrix $f(A,x)$ (matrix A, scalar x) to a double matrix $f(A,B)$ (two matrices A,B) as in Eq. (C4). To calculate

$$\int_{-\infty}^{\infty} \frac{d\omega'}{2\pi} \phi^{km}(\vec{q}', \omega')\phi^{ln}(\vec{q}-\vec{q}', \omega-\omega') = i\sqrt{\chi^k_{\vec{q}'}\chi^m_{\vec{q}'}\chi^l_{\vec{q}-\vec{q}'}\chi^n_{\vec{q}-\vec{q}'}}\{f_{km}[g'(\vec{q}'), \omega\mathbf{1} + ig'(\vec{q}-\vec{q}')]\}^{ln}, \quad \text{(C12)}$$

we therefore have to calculate the quotient of two matrices [which can be achieved applying Eq. (C8)], which consist of polynomials of the matrix $g'(\vec{q}-\vec{q}')$ [cf. Eq. (C6) where the scalar x now has to be replaced by the matrix B]. The coefficients of these polynomials are given by matrix elements of the matrix $g'(\vec{q}')$.

APPENDIX D: DIAGONALIZING MATRIX IN LIMITING CASES

In the following, we describe four limiting cases where the diagonalizing matrix $T_{\vec{q}}$ (50) can be determined *a priori* at least approximately.

1. Small damping

The first limiting case we deal with is an expansion for small linewidths, i.e., $\Gamma^{ij} \ll \omega_{\vec{q}}$. Therefore, to leading order $T_{\vec{q}}$ is given by the matrix $T^{\omega}_{\vec{q}}$ which just diagonalizes the frequency matrix $C_{\vec{q}}$ of Eq. (49). In this case, $T_{\vec{q}}$ is unitary, independent of frequency and given by

$$T^{\omega}_{\vec{q}} = \begin{pmatrix} 0 & \frac{1}{\sqrt{2}} & \frac{1}{\sqrt{2}} \\ \cos\gamma & -\frac{i}{\sqrt{2}}\sin\gamma & \frac{i}{\sqrt{2}}\sin\gamma \\ -\sin\gamma & -\frac{i}{\sqrt{2}}\cos\gamma & \frac{i}{\sqrt{2}}\cos\gamma \end{pmatrix}. \quad \text{(D1)}$$

The angle γ has been defined in Eq. (B5). To leading order, the eigenvalues in Eq. (51) are the diagonal elements of G'^{ab}.

2. Isotropic case

The above formula Eq. (D1) can also be used in the isotropic limit without dipolar interaction. Then we have $\gamma \equiv 90°$, which yields

$$T^{0}_{\vec{q}} = \begin{pmatrix} 0 & \frac{1}{\sqrt{2}} & \frac{1}{\sqrt{2}} \\ 0 & -\frac{i}{\sqrt{2}} & \frac{i}{\sqrt{2}} \\ -1 & 0 & 0 \end{pmatrix}, \quad y = 0. \quad \text{(D2)}$$

This formula for the isotropic case, however, is valid in general, not only for small damping. Note that this corresponds to a decomposition into modes S^z, S^+, and S^-, since the static susceptibility is diagonal in Cartesian coordinates in this case. Again, $T_{\vec{q}}$ is unitary and does not depend on frequency. The eigenvalues in Eq. (51) are strictly given by the diagonal elements of G'^{ab}. The frequency matrix, the damping matrix as well as the relaxation function are diagonal simultaneously. Because of Eq. (53) the quantities $\tilde{w}^{ab}_c$, $\vec{u}^0$,

and $\vec{w}^0$ are identical with w_c^{ab}, $\vec{u}$, and $\vec{w}$, respectively. This simplifies the expressions for w_c^{ab} Eq. (65) considerably

$$|w_L^{TT^*}(x,y,\vartheta,\vec{\kappa})|=|2\kappa\eta-1|\sqrt{1+x^2},$$

$$|w_T^{LT}(x,y,\vartheta,\vec{\kappa})|=|2\kappa\eta-1|\,\frac{\kappa}{\sqrt{\kappa^2+x^2}},$$

$$|w_{T*}^{LT*}(x,y,\vartheta,\vec{\kappa})|=|w_T^{LT}(x,y,\vartheta,\vec{\kappa})|,$$

$$w_c^{ab}(x,y,\vartheta,\vec{\kappa})=0 \quad \text{all other cases } (a\leqslant b), \tag{D3}$$

in accordance with Ref. 11.

3. Limiting case $T=T_c$

At T_c it is known that the relevant coordinate system is oriented along the direction of the wave vector.[11] By using the eigenvectors of the static susceptibility as a basis, this feature is taken into account automatically, and the resulting diagonalizing matrix, in accordance with Ref. 11, is given by

$$T_{\vec{q}}^{T_c}=\begin{pmatrix}0&1&0\\0&0&1\\1&0&0\end{pmatrix}, \quad T\geqslant T_c\,. \tag{D4}$$

This is basically the identity matrix, permutated, because the $(i=3)$ mode corresponds to the $(a=L)$ mode and so on. As in the isotropic case, the above transformation is unitary and frequency independent and it diagonalizes exactly all quantities in question.

4. Large damping

The opposite case to that outlined in Appendix D 1 is characterized by $\Gamma^{ij}\gg\omega_{\vec{q}}$. It contains as a limiting case $T=T_c$, since there the frequency matrix vanishes and the condition $\Gamma^{ij}\gg\omega_{\vec{q}}$ is always fulfilled. Therefore, we can suppose that also for small deviations from T_c or equivalently for frequency small compared with the damping, Γ is still nearly diagonal. Off diagonal elements of M (49) then are introduced solely by the frequency matrix

$$[M^{-1}]^{ij}\approx[M^{T_c}]^{ij}\coloneqq[-i\Gamma+C_{\vec{q}}]^{ij}$$
$$=\begin{pmatrix}-i\Gamma_1 & i\omega_{\vec{q}}\sin\gamma & i\omega_{\vec{q}}\cos\gamma\\ -i\omega_{\vec{q}}\sin\gamma & -i\Gamma_2 & 0\\ -i\omega_{\vec{q}}\cos\gamma & 0 & -i\Gamma_3\end{pmatrix}. \tag{D5}$$

At T_c the eigenvalues Γ_1 and Γ_2 are degenerate $(=\Gamma_T)$ while $\Gamma_3=\Gamma_L$ is in general different. Expanding the associated eigenvalue equation up to terms of $O(\omega_{\vec{q}})$ is equivalent to replacing the matrix M^{T_c} by

$$[M^{T_c}]^{ij}\approx\begin{pmatrix}-i\Gamma_T & i\omega_{\vec{q}}\sin\gamma & 0\\ -i\omega_{\vec{q}}\sin\gamma & -i\Gamma_T & 0\\ 0 & 0 & -i\Gamma_L\end{pmatrix}. \tag{D6}$$

Correspondingly, the eigenvalues of M^{T_c} are given by

$$\begin{aligned}\omega_1&=-i\Gamma_T+\omega_{\vec{q}}\sin\gamma+O(\omega_{\vec{q}}^2),\\ \omega_2&=-i\Gamma_T-\omega_{\vec{q}}\cos\gamma+O(\omega_{\vec{q}}^2),\\ \omega_3&=-i\Gamma_L+O(\omega_{\vec{q}}^2),\end{aligned} \tag{D7}$$

and the eigenvectors by

$$\vec{n}_{1/2}=\frac{1}{\sqrt{2}}\begin{pmatrix}1\\ \mp i\\ 0\end{pmatrix}+O(\omega_{\vec{q}}), \quad \vec{n}_3=\begin{pmatrix}0\\0\\1\end{pmatrix}+O(\omega_{\vec{q}}). \tag{D8}$$

Choosing a phase factor -1 in the eigenvector $\vec{n}_3$, we get the following transformation matrix:

$$T_{\vec{q}}^{\Gamma}=\begin{pmatrix}0 & \frac{1}{\sqrt{2}} & \frac{1}{\sqrt{2}}\\ 0 & -\frac{i}{\sqrt{2}} & \frac{i}{\sqrt{2}}\\ -1 & 0 & 0\end{pmatrix}. \tag{D9}$$

Remarkably, this is identical to $T_{\vec{q}}^0$, Eq. (D2). It can also be used at T_c, since there the transverse modes 1 and 2 or equivalently T and T^* are degenerate and can be superimposed linearly. Equation (D9) can therefore equivalently replace Eq. (D4).

[1] P. Böni, J. L. Martínez, and J. M. Tranquada, Phys. Rev. B **43**, 575 (1991).
[2] P. Böni, H. A. Mook, J. L. Martínez, and G. Shirane, Phys. Rev. B **47**, 3171 (1993).
[3] P. Böni, Y. Endoh, H. A. Graf, M. Hennion, J. L. Martínez, and G. Shirane, Physica B **213&214**, 303 (1995); P. Böni, M. Hennion, and J. L. Martinez, Phys. Rev. B **52**, 10 142 (1995).
[4] J. Kötzler, D. Görlitz, F. Mezei, and B. Farago, Europhys. Lett. **1**, 675 (1986).
[5] D. Görlitz, J. Kötzler, F. J. Bermejo, P. Böni, and J. L. Martínez, Physica B **180&181**, 214 (1992).
[6] F. Mezei, Int. J. Mod. Phys. B **7**, 2885 (1993).

[7] M. Grahl, D. Görlitz, J. Kötzler, T. Lange, and I. Seßler, J. Appl. Phys. **69**, 6179 (1991); D. Görlitz, J. Kötzler, and T. Lange, J. Magn. Magn. Mater. **104-107**, 339 (1992).
[8] J. Kötzler, E. Kaldis, G. Kamleiter, and G. Weber, Phys. Rev. B **43**, 11 280 (1991); R. Dombrowski, D. Görlitz, J. Kötzler, and C. Marx, J. Appl. Phys. **75**, 6054 (1994); J. Kötzler, D. Görlitz, M. Hartl, and C. Marx, IEEE Trans. Magn. **30**, 828 (1994).
[9] M. W. Pieper, J. Kötzler, and K. Nehrke, Phys. Rev. B **47**, 11 962 (1993).
[10] J. Kötzler, D. Görlitz, R. Dombrowski, and M. Pieper, Z. Phys. B **94**, 9 (1994).
[11] E. Frey and F. Schwabl, Z. Phys. B **71**, 355 (1988); **76**, 139(E) (1989).
[12] E. Frey, F. Schwabl, and S. Thoma, Phys. Rev. B **40**, 7199 (1989).
[13] E. Frey and F. Schwabl, Adv. Phys. **43**, 577 (1994).
[14] I. D. Lawrie, J. Phys. A **14**, 2489 (1981); **18**, 1141 (1985).
[15] U. C. Täuber and F. Schwabl, Phys. Rev. B **46**, 3337 (1992).
[16] A. Z. Patashinskii and V. L. Pokrovskii, Sov. Phys. JETP **37**, 733 (1973); V. L. Pokrovsky, Adv. Phys. **28**, 595 (1979).
[17] H. S. Toh and G. A. Gehring, J. Phys.: Condens. Matter **2**, 7511 (1990).
[18] S. W. Lovesey and K. N. Trohidou, J. Phys.: Condens. Matter **3**, 1827 (1991); **3**, 5255(E) (1991).
[19] A. Cuccoli, S. W. Lovesey, G. Pedrolli, and V. Tognetti, J. Phys.: Condens. Matter **5**, 3241 (1993).
[20] U. C. Täuber, F. Schwabl, Phys. Rev. B **48**, 186 (1993).
[21] H. Schinz and F. Schwabl, preceding paper, Phys. Rev. B **57**, 8430 (1998).
[22] S. W. Lovesey, Europhys. Lett. **15**, 63 (1991); K. N. Trohidou and S. W. Lovesey, J. Phys.: Condens. Matter **5**, 1109 (1993).
[23] B. P. Toperverg and A. G. Yashenkin, Phys. Rev. B **48**, 16 505 (1993); B. P. Toperverg, V. V. Deriglazov, and V. E. Mikhailova, Physica B **183**, 326 (1993).
[24] S. V. Maleev, Sov. Sci. Rev. Sect. A: Phys. Rev. **8**, 323 (1987).
[25] R. Raghavan and D. L. Huber, Phys. Rev. B **14**, 1185 (1976).
[26] S. W. Lovesey, J. Phys.: Condens. Matter **5**, L251 (1993).
[27] S. Ma and G. F. Mazenko, Phys. Rev. B **11**, 4077 (1975).
[28] L. Sasvári, J. Phys. C **10**, L633 (1977).
[29] B. I. Halperin and P. C. Hohenberg, Phys. Rev. **188**, 898 (1969); **177**, 952 (1969).
[30] The state of spin-wave theory as from 1966 is described in F. Keffer, *Spin Waves in S. Flügge, Handbuch der Physik*, Bd. XVIII/2, *Ferromagnetismus* (Springer, Berlin, 1966).
[31] V. G. Vaks, A. I. Larkin, and S. A. Pikin, Sov. Phys. JETP **26**, 647 (1968).
[32] J. Villain, Solid State Commun. **8**, 31 (1970).
[33] J. Villain, in *Critical Phenomena in Alloys, Magnets and Superconductors*, edited by R. E. Mills, E. Ascher, R. E. Jaffee (McGraw-Hill, New York, 1971) Sec. 423.
[34] V. N. Kashcheev and V. N. Krivoglaz, Sov. Phys. Solid State **3**, 1117 (1961); A. B. Harris, Phys. Rev. **175**, 674 (1968).
[35] F. Schwabl and K. H. Michel, Phys. Rev. B **2**, 189 (1970).
[36] F. Schwabl, Z. Phys. **13**, 246 (1971).
[37] K. Chen and D. P. Landau, Phys. Rev. B **49**, 3266 (1994).
[38] M. E. Fisher and A. Aharony, Phys. Rev. Lett. **30**, 559 (1973); Phys. Rev. B **8**, 3323 (1973); A. Aharony, *ibid.* **8**, 3342 (1973).
[39] A. Yaouanc, P. Dalmas de Réotier, and E. Frey, Phys. Rev. B **47**, 796 (1993).
[40] M. J. Fixman, J. Chem. Phys. **33**, 1363 (1960); **36**, 1961 (1962).
[41] K. Kawasaki, J. Phys. Chem. Solids **28**, 1277 (1967).
[42] K. Kawasaki, Ann. Phys. (N.Y.) **61**, 1 (1970).
[43] W. Götze and L. Sjögren, Rep. Prog. Phys. **55**, 241 (1992).
[44] T. Hwa and E. Frey, Phys. Rev. A **44**, R7873 (1991).
[45] P. Le Doussal and L. Radzihovsky, Phys. Rev. Lett. **69**, 1209 (1992).
[46] T. M. Fischer, E. Frey, and F. Schwabl, Phys. Lett. A **146**, 457 (1990).
[47] S. Thoma, E. Frey, and F. Schwabl, Phys. Rev. B **43**, 5831 (1991).
[48] K. Kawasaki, in *Phase Transitions and Critical Phenomena*, edited by C. Domb and M. S. Green (Academic, New York, 1976), Vol. 5a, and references therein.
[49] E. Fick and G. Sauermann, *The Quantum Statistics of Dynamical Processes*, translated by W. D. Brewer (Springer, Berlin, 1980).
[50] S. W. Lovesey, *Condensed Matter Physics–Dynamic Correlations*, 2nd ed. (Benjamin, Menlo Park, CA, 1986).
[51] D. Forster, *Hydrodynamic Fluctuations, Broken Symmetry and Correlation Functions* (Benjamin, Menlo Park, CA, 1975).
[52] H. Mori, Prog. Theor. Phys. **33**, 423 (1965).
[53] R. Zwanzig, Phys. Rev. **124**, 983 (1961).
[54] T. Holstein and H. Primakoff, Phys. Rev. **58**, 1098 (1940).
[55] H. B. Callen, Phys. Rev. **130**, 890 (1963).
[56] P. C. Hohenberg and B. J. Halperin, Rev. Mod. Phys. **49**, 435 (1977).
[57] S. Ma, *Modern Theory of Critical Phenomena* (Benjamin, Reading, MA, 1976).
[58] H. Schinz and F. Schwabl, J. Magn. Magn. Mater. **140–144**, 1527 (1995).
[59] H. Schinz and F. Schwabl, following paper, Phys. Rev. B **57**, 8456 (1998).
[60] R. Haussmann, Z. Phys. B **79**, 143 (1990).
[61] L. Passell, O. W. Dietrich, and J. Als-Nielsen, Phys. Rev. B **14**, 4897 (1976); J. Als-Nielsen, O. W. Dietrich, and L. Passell, *ibid.* **14**, 4908 (1976); O. W. Dietrich, J. Als-Nielsen, and L. Passell, *ibid.* **14**, 4923 (1976).
[62] F. Mezei, J. Magn. Magn. Mater. **45**, 67 (1984).
[63] P. Böni and G. Shirane, Phys. Rev. B **33**, 3012 (1986).
[64] S. Schorr (private communication).
[65] P. Böni (private communication).